THE ROYAL SOCIETY

Published online 7 July 2004

Protein hydration dynamics in solution: a critical survey

Bertil Halle

Department of Biophysical Chemistry, Lund University, SE-22100 Lund, Sweden (*bertil.halle@bpc.lu.se*)

The properties of water in biological systems have been studied for well over a century by a wide range of physical techniques, but progress has been slow and erratic. Protein hydration—the perturbation of water structure and dynamics by the protein surface—has been a particularly rich source of controversy and confusion. Our aim here is to critically examine central concepts in the description of protein hydration, and to assess the experimental basis for the current view of protein hydration, with the focus on dynamic aspects. Recent oxygen-17 magnetic relaxation dispersion (MRD) experiments have shown that the vast majority of water molecules in the protein hydration layer suffer a mere twofold dynamic retardation compared with bulk water. The high mobility of hydration water ensures that all thermally activated processes at the protein–water interface, such as binding, recognition and catalysis, can proceed at high rates. The MRD-derived picture of a highly mobile hydration layer is consistent with recent molecular dynamics simulations, but is incompatible with results deduced from intermolecular nuclear Overhauser effect spectroscopy, dielectric relaxation and fluorescence spectroscopy. It is also inconsistent with the common view of hydration effects on protein hydrodynamics. Here, we show how these discrepancies can be resolved.

Keywords: magnetic relaxation dispersion; nuclear Overhauser effect; dynamic Stokes shift; dielectric relaxation; protein hydrodynamics; water dynamics

1. INTRODUCTION

The proteins that make up the molecular machinery of life have been perfected by several billion years of evolution that, as far as we know, has taken place exclusively in aqueous environments. During this evolutionary process, proteins have adapted to and exploited the unique physical properties of liquid water (Eisenberg & Kauzmann 1969) in many ways. Protein–water interactions thus shape the free energy landscape that governs the folding, structure and stability of proteins (Kauzmann 1959; Dill 1990). Moreover, the functional processes mediated by proteins, such as binding, recognition and catalysis, often involve specific interactions with individual water molecules (Meyer 1992; Williams *et al.* 1994; Baker 1995).

The properties of water in biological systems have been studied for well over a century by a wide range of physical techniques (Kuntz & Kauzmann 1974; Rupley & Careri 1991). However, none of these techniques provides the spatial and temporal resolution required to directly probe water molecules interacting with the surface of a protein in aqueous solution. The current view of the structure and dynamics of protein hydration is therefore based on more or less model-dependent interpretations of experimental data. Given the high complexity of proteins and the incomplete understanding of bulk liquid water and of small-molecule hydration, it is perhaps not surprising that progress within the field of protein hydration has been slow and erratic. Regrettably, the increasing sophistication of experimental tools used to study protein hydration tends to fragment the research field into method-oriented subspecialties that rarely confront each other.

The present review is an attempt to critically examine the experimental basis of the current (multiple) views on protein hydration, with an emphasis on the dynamic aspects. A recurring theme in the field of protein hydration is that first appearances are usually deceptive: nearly every new experimental technique that has been applied to protein hydration in solution has gone through a painful gestation period of interpretational controversy. To make progress, it is therefore helpful to adopt a sceptical attitude. Our scope here is necessarily selective, with respect to both methods and systems. Although several methods are discussed, we emphasize magnetic-relaxation techniques and, in particular, MRD. Furthermore, we focus on surface hydration of native proteins in aqueous solution, largely bypassing the important topics of internal water molecules (Halle 1998) and the role of water in protein folding and stability (Halle *et al.* 2004).

2. PROTEIN HYDRATION DEFINED

The term hydration is commonly used to cover two different phenomena: (i) the total interaction of a solute with its aqueous solvent environment; and (ii) the perturbation of the structure and dynamics of bulk water caused by the interaction with the solute. Here, we use hydration in the latter, more restrictive sense. The water molecules that interact with a protein can, with little ambiguity, be classified as internal or external. Internal water molecules

One contribution of 16 to a Discussion Meeting Issue 'The molecular basis of life: is life possible without water?'.

© 2004 The Royal Society

occupy cavities within the protein and are present in most globular proteins (Williams *et al.* 1994). They are conserved to the same extent as the amino acid sequence and must therefore be essential for function (Baker 1995). For most purposes, internal water molecules are best regarded as an integral part of the protein, even though they exchange with external water molecules, typically on a time-scale of 0.1–10 μs (Halle 1998).

The vast majority of all studies of protein hydration have been concerned with the water molecules that interact with the external protein surface. This interaction modifies the structure and dynamics of water near the surface, and the spatial range of this perturbation has been a contentious issue. Such controversies can often be traced back to a too literal interpretation of analogies and metaphors used to illustrate particular aspects of bulk water structure (*in lieu* of a quantitative molecular model). For example, the first studies to invoke long-range hydration structures in biological systems (Jacobson 1953; Jacobson *et al.* 1954) were inspired by a structural model of bulk water based on a deformed ice lattice, thought to be stabilized by substrates with a matching complement of hydrogen-bonding sites (Forslind 1952; Samoilov 1957). Other advocates of 'frozen' hydration layers around biopolymers (Klotz 1958) were apparently inspired by the 'iceberg' metaphor used to illustrate structural aspects of hydrophobic hydration (Frank & Evans 1945). Hydration structures with a range of several 100 Å ($1\ \text{Å} = 1 \times 10^{-10}$ m) were also postulated by arguing that zwitterionic surfaces can polarize water dipoles in a cooperative manner, forming 'polarized multilayers' that were claimed to account for the ionic asymmetry of intracellular and extracellular water without the need to invoke active ion transport (Ling 1962). Similar ideas have been championed since the 1960s by a persevering minority of predominantly biomedical researchers, maintaining that the structure of so-called 'biological water' differs essentially from that of simple aqueous solutions (Hazlewood 2001). Similarly, a surface-induced water structure of very long range was postulated in the colloid field, with apparent 'thermal anomalies' in various observables taken as evidence for structural transitions involving extensive regions of ordered so-called 'vicinal water' (Drost-Hansen 2001). The ultimate form of structured water was, of course, polywater. The remarkable history of this experimental artefact is a sobering lesson (Franks 1981).

Protein–water interactions are of similar strength as water–water interactions and are therefore not expected to induce extensive structural perturbations. Indeed, magnetic relaxation (Halle 1998) and computer simulation (Abseher *et al.* 1996; Makarov *et al.* 2000; Marchi *et al.* 2002) studies indicate that only water molecules in direct contact with the protein surface are significantly perturbed. Moreover, the vast majority of water molecules in this hydration layer are not more perturbed than water molecules in contact with small solutes (Modig *et al.* 2004). Nevertheless, these water molecules are often referred to as 'bound'. This term aptly describes the strongly exothermic adsorption of water molecules on the surface of a dry (vaporized or lyophilized) protein (Rupley & Careri 1991), but it is misleading when applied to a protein immersed in an aqueous solvent. Water molecules in the hydration layer of a dissolved protein are not bound in a thermodynamic or kinetic sense. It is therefore not physically meaningful to describe protein hydration in terms of an equilibrium between bound and free water, as is commonly done (Nandi & Bagchi 1997, 1998; Bhattacharyya & Bagchi 2000; Nandi *et al.* 2000). In the absence of cosolvents, every exposed hydration site is virtually always occupied by a water molecule, and the transition of a water molecule from the 'bound' to the 'free' state is invariably accompanied by the reverse transition of another water molecule. In other words, we are dealing with a symmetric exchange process for which the equilibrium constant is trivially equal to one. Water simply fills the available space.

3. STRUCTURE VERSUS DYNAMICS

The dynamic aspect of protein hydration is often discussed in terms of the residence time of water molecules. For a strongly bound ligand or an internal water molecule, the mean residence time is a well-defined quantity, given by the inverse of the first-order dissociation rate constant. When applied to water molecules in the hydration layer, however, the residence time concept is problematic. Such residence times cannot be directly determined by any known experimental technique. Furthermore, residence times computed from molecular dynamics trajectories depend sensitively on how one treats the frequent recrossings of the relatively low potential (of mean force) barrier (Impey *et al.* 1983). A more appropriate measure of the local dynamic perturbation of hydration water is the ratio, $D_{\text{R,bulk}}/D_{\text{R,hyd}}$, of the rotational diffusion coefficients of bulk water and hydration water or, equivalently, the ratio of the corresponding rotational correlation times. This quantity is experimentally accessible (see § 5a) and can readily be obtained from simulations of molecular dynamics. Because rotational and translational water motions are both governed by the rate at which hydrogen bonds are broken and reformed (Halle 1998; Marchi *et al.* 2002; Geiger *et al.* 2003), the rotational retardation factor, $D_{\text{R,bulk}}/D_{\text{R,hyd}}$, should not differ much from the translational retardation factor, $D_{\text{T,bulk}}/D_{\text{T,hyd}}$. However, the rotational retardation factor has the advantage of reflecting a more localized motion.

Failure to distinguish thermodynamic and structural properties from dynamic properties may be the most common source of confusion in the molecular sciences. For any equilibrium system governed by classical equations of motion (as assumed in all forcefield-based molecular dynamics simulations), excess (non-ideal) thermodynamic and structural properties are rigorously independent of dynamics. Properties like entropy and flexibility are often discussed in terms of thermal motion, and equilibrium constants can be viewed as the result of opposing rate processes. However, excess thermodynamic and structural properties do not depend on the rates of molecular motions. For example, the residence time of a water molecule in the hydration layer tells us nothing about its effect on the thermodynamic stability of the protein, or about the affinity or recognition selectivity of association processes involving this part of the surface. Conversely, mean atomic displacement factors, as determined by X-ray diffraction, carry no dynamic information (Halle 2002). Regrettably, the word 'dynamics' is widely used to describe disorder and

flexibility in biomolecular systems. However, these equilibrium properties are completely determined by the interaction energy and are entirely independent of the forces (Greek: *dynamis*) that produce motions.

On the time-scales of interest in connection with hydration phenomena, molecular motions are frictionally over-damped and can often be modelled as a diffusion process in a potential (of mean force). Motional rates are then determined mainly by the height of barriers and saddle points on the energy surface, whereas structure and thermodynamics are governed mainly by local minima. Accordingly, water residence times are determined not so much by attractive interactions (in the energy minimum) as by the lack of such interactions (at the barrier top). The million-fold increase in the mobility of water molecules on melting of ice cannot be explained by broken hydrogen bonds (most of which are intact in the liquid). Instead, the remarkably fast molecular motions in liquid water result from cooperative rearrangements of the disordered hydrogen-bond network, allowing water molecules to rotate or translate without having to pass through a 'transition state', where all hydrogen bonds are broken (Geiger *et al.* 2003). An unusually long residence time for a hydration water molecule, therefore, does not indicate particularly strong protein–water interactions, but rather a topography that prevents the water molecule from exchanging by a cooperative mechanism. The simplest example of such restrictive topography is a deep pocket on the protein surface. Water molecules located in surface pockets typically have the same number (two or three) of hydrogen bonds with the protein as they would have with other water molecules in the bulk solvent. However, to leave the pocket, the water molecule has to pass through a high-energy state where the water–protein hydrogen bonds must be broken before new water–water hydrogen bonds can be formed. In biological water channels (aquaporins), such high energy barriers are avoided by a suitable arrangement of hydrogen-bond partners along the channel (Fujiyoshi *et al.* 2002).

4. STRUCTURE OF PROTEIN HYDRATION

When Irwin Kuntz and Walter Kauzmann wrote their classic review on protein hydration 30 years ago (Kuntz & Kauzmann 1974), the three-dimensional structures of about 10 proteins were known. In several of these, electron density peaks within small cavities had been tentatively modelled as water molecules (Drenth *et al.* 1971; Quiocho & Lipscomb 1971). The subsequent rapid growth of the Protein Data Bank, now holding some 20 000 protein crystal structures, has confirmed this interpretation and established internal water molecules as a generic feature of globular proteins, with an average of one internal water molecule per 25 amino acid residues in monomeric globular proteins (Williams *et al.* 1994). This massive body of structural data also contains information about surface hydration. However, the crystallographic localization of exposed hydration sites relies on refinement protocols that are, to some extent, subjective (Badger 1997). For example, in a comparison of four independent determinations of the same crystal form of interleukin 1β, only 29 hydration sites coincided to within 1 Å among the four structures and many of these were internal sites (Ohlendorf 1994).

Even if hydration sites could be identified accurately, protein hydration in the crystal is not the same as in solution. For small proteins, 30–40% of the solvent-accessible surface is usually buried at crystal contacts (Islam & Weaver 1990), where water molecules often mediate protein–protein interactions. Furthermore, salting-out agents and cryoprotectants, usually present at high concentration in the mother liquor, permeate the crystal and may perturb or even be mistaken for hydration sites (Frey 1994; Baker 1995). The importance of crystal-specific hydration features can be assessed by comparing the hydration sites of the same protein in different crystal forms, or at non-equivalent positions in the asymmetric unit. In such comparisons, it is usually found that less than half of the reported hydration sites are conserved (Baker 1995). For example, only 12 external hydration sites on the protein BPTI were found to be conserved among three crystal forms (Wlodawer *et al.* 1987)

Strictly speaking, diffraction methods do not monitor water molecules. Rather, resolved maxima in the electron-density map locate reproducibly occupied hydration sites. Crystallographers frequently refer to such sites as 'tightly bound' water molecules. However, diffraction data do not tell us anything about the energetics of water–protein interactions or about the kinetics of water exchange between hydration sites and bulk solvent. In general, diffraction (or scattering) experiments provide information about generic spatial correlations, that is, the probability of finding any molecule of species A at a certain distance from any molecule of species B (which may be the same as A). From X-ray diffraction on bulk water, one obtains a radially averaged pair correlation function with a strong peak at 2.8 Å, corresponding to the most probable nearest-neighbour oxygen–oxygen separation (Eisenberg & Kauzmann 1969). Similarly, X-ray diffraction on a protein crystal gives information about protein–water correlations. The fact that the protein molecule is stationary while the reference water molecule, in the case of bulk water, is mobile, is irrelevant here. The only essential difference is the absence of long-range order in the liquid, which eliminates the angular information. Therefore, just as in the liquid, we expect a peak in the pair correlation functions between protein atoms and water oxygens. Such a peak would occur even in the absence of other protein–water interactions than the excluded volume. If we define a local water density by integrating the pair correlation function over the first layer, we will find that it exceeds the bulk density. This is also true for hard spheres in contact with a hard wall (Snook & Henderson 1978). For proteins, solution X-ray and neutron scattering indicates that the density excess in the hydration layer amounts to 10–15% (Svergun *et al.* 1998; Seki *et al.* 2002), and computer simulations have confirmed this (Merzel & Smith 2002; Seki *et al.* 2002). Simple packing constraints may also be the main cause of the observed dependence of the local water density on the curvature of the protein surface, with a higher density near the concave surface regions (Gerstein & Chothia 1996; Merzel & Smith 2002).

Within the past decade, protein crystallography has been transformed: today, *ca.* 90% of all protein crystal structures are determined at cryogenic temperatures, some

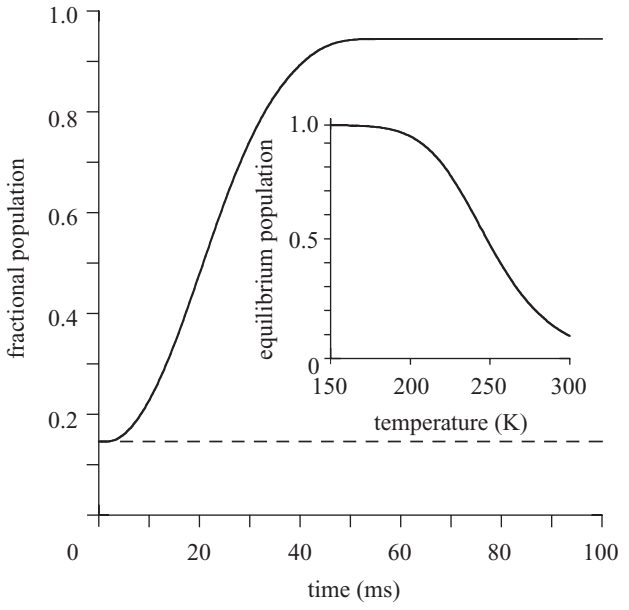

Figure 1. Calculated time evolution of the fractional population in the low-temperature state of a two-state equilibrium during flash-cooling of a spherical protein crystal (0.5 mm radius, thermal diffusivity $1.2 \times 10^{-7}\ m^2\ s^{-1}$) from 293 K to 77 K. The equilibrium population, corresponding to $\Delta H = 25\ kJ\ mol^{-1}$ and $\Delta S = 100\ J\ K^{-1}\ mol^{-1}$, is shown in the insert. The state interconversion kinetics are modelled with an activation enthalpy of $40\ kJ\ mol^{-1}$, the diffusion coefficient of water, and a state lifetime of 10 ns at 293 K. The equilibrium is quenched after 47 ms when the crystal temperature is 202 K, corresponding to 95% population in the low-temperature state (compared with 15% at 293 K). The time-dependent temperature is averaged over the middle one-third of the crystal volume (Halle 2004).

200 K below the physiological temperature range (Garman 2003). Cryocrystallography evolved primarily as a means to combat radiation damage to crystals from intense synchrotron X-ray beams, based on the idea that radiation-induced free radicals cannot damage the biomolecule once they are trapped in the vitrified bulk solvent within the crystal (Garman & Schneider 1997). The insufficiently appreciated price for this protection is the introduction of structural cryo-artefacts.

In the limit of infinitely fast cooling, the system would be quenched into an amorphous solid (glass) state reflecting the room-temperature equilibrium Boltzmann distribution of conformational substates. However, this adiabatic limit is not realized in practical flash-cooling protocols, which, even for small protein crystals, yield characteristic cooling times on the order of 0.1–1 s (Kriminski *et al.* 2003). There is thus ample time for thermal averaging during the cooling process. The structural changes expected during flash cooling of a protein crystal have recently been calculated for a temperature-dependent two-state equilibrium (Halle 2004). This analysis indicates that many degrees of freedom are quenched at temperatures near 200 K, where local conformational and association equilibria may be strongly shifted towards low-enthalpy states (see figure 1). Delayed quenching and consequent cryo-artefacts should be most pronounced in the interfacial region. This is usually where the biologically interesting recognition, binding and catalytic events occur.

In ultrahigh-resolution protein structures obtained at cryogenic temperature, extensive hydrogen-bond networks of fused 5-, 6- and 7-membered rings of water molecules are commonly observed (Nakasako 1999; Esposito *et al.* 2000; Teeter *et al.* 2001). If such hydration structures were present at room temperature, water motions in the hydration layer would be strongly retarded compared with bulk water. However, ^2H and ^{17}O MRD studies indicate a mere twofold dynamic retardation for the vast majority of water molecules in the hydration layer of proteins (see § 5a). For the small protein crambin, where ultrahigh-resolution structures have been reported at several temperatures from 100 K to 293 K, the 6- and 7-membered rings disappear above 200 K (Teeter *et al.* 2001), suggesting that they are, in fact, cryo-artefacts.

The hydration of non-polar cavities and channels in proteins may also be susceptible to cryo-artefacts. This is probably an entropy-driven process (Denisov *et al.* 1997*a*), with the low-temperature state corresponding to an empty cavity. For example, water molecules in the central channel of bacteriorhodopsin are thought to play an active role in the proton-translocation mechanism (Lanyi 2000). The high-resolution cryostructure of bacteriorhodopsin shows a network of water molecules on the highly polar, extracellular side of the retinal molecule, but a corresponding network that could transport the proton through the mainly non-polar cytoplasmic half of the channel is not evident (Luecke *et al.* 1999). ^2H and ^{17}O MRD measurements are consistent with more water molecules in the channel than seen in the crystal structure and show that these water molecules exchange with bulk water on a microsecond time-scale at 277 K (Gottschalk *et al.* 2001). With a probable quenching temperature of *ca.* 200 K, some of the channel waters may have been expelled during flash cooling.

5. MAGNETIC RELAXATION AS A PROBE OF PROTEIN HYDRATION DYNAMICS

Magnetic relaxation methods have long played a leading role in the study of protein hydration dynamics. Early observations of an enhanced water ^1H relaxation rate in protein solutions were attributed to a few water molecules rigidly bound to (and thus tumbling with) the protein, but exchanging rapidly with the remaining bulk-like water (Daszkiewicz *et al.* 1963). On the basis of relaxation data at two magnetic fields, a three-state model was proposed that also incorporated hydration water with rotational dynamics intermediate between rigidly bound and bulk water (Caputa *et al.* 1967). Although these early workers were on the right track, it would take three decades of erratic progress to unravel the essential molecular mechanisms of water relaxation in aqueous protein solutions. Three decisive elements can be identified in the ensuing development.

Measurements of the frequency dependence of the longitudinal relaxation rate R_1, known as MRD, are required to determine the shape of the spectral density function that carries the molecular-level information. Specialized techniques for relaxation–dispersion measurements were developed in several laboratories in the late 1960s (Redfield *et al.* 1968; Florkowski *et al.* 1969; Kimmich & Noack 1970*a*), and were soon applied to the

protein-hydration problem (Koenig & Schillinger 1969; Blicharska *et al.* 1970; Kimmich & Noack 1970*b*). Extending over four decades in frequency, the new water ^{1}H MRD data represented an experimental breakthrough, but, as regards the interpretation, they raised more questions than they answered. In their review, Kuntz & Kauzmann (1974) linked the ^{1}H dispersions observed by these groups to the newly discovered internal water molecules in proteins. Unfortunately, this prescient idea did not catch on.

For a long time, further progress was impeded by the failure to appreciate the confounding effect of labile hydrogens in the protein that, depending on pH, exchange rapidly with water hydrogens, thus mimicking long-lived water molecules. This obstacle was circumvented by using the ^{17}O isotope to exclusively monitor the behaviour of water molecules (Halle *et al.* 1981). The third essential step in uncovering the molecular basis of the frequency-dependent water relaxation enhancement in protein solutions was the availability of high-resolution protein crystal structures and genetically engineered proteins, which paved the way for decisive ^{17}O MRD experiments designed to identify the internal water molecules responsible for the relaxation dispersion (Denisov & Halle 1994; Denisov *et al.* 1996).

In parallel with the development of the MRD method, other events took place that led to a different NMR approach to protein hydration, based on incoherent magnetization transfer between water and protein protons by cross-relaxation and chemical exchange. The transfer of magnetization between two non-equivalent dipole-coupled nuclei as a result of dipolar cross-relaxation, known as the NOE, has long been exploited in structural and dynamical NMR studies (Neuhaus & Williamson 2000). Double-resonance experiments demonstrating NOE-induced saturation transfer from water protons to specific protons in oligopeptides in solution were reported 30 years ago (Pitner *et al.* 1974; Glickson *et al.* 1976) and were soon followed by demonstrations of saturation transfer between water and protein protons (Stoesz *et al.* 1978; Akasaka 1979). The latter observations were taken as evidence for long (greater than 1 ns) water residence times at the protein surface, as previously inferred (also incorrectly) from ^{1}H MRD data. These pioneering NOE studies of protein hydration suffered from the same interpretational problems as the early ^{1}H MRD studies: the confounding effects of labile hydrogen exchange (Van de Ven *et al.* 1988) and the failure to appreciate the crucial role of internal water molecules.

With the advent of 2D NMR spectroscopy in the 1980s (Ernst *et al.* 1987), these one-dimensional magnetization-transfer experiments evolved into the more powerful modern 2D spectroscopies, including NOESY, ROESY and a host of related pulse schemes for probing magnetization transfer by cross-relaxation and/or chemical exchange. Two-dimensional NOESY studies of water cross-peaks were soon reported for oligopeptides and proteins (Schwartz & Cutnell 1983; Dobson *et al.* 1986; Van de Ven & Hilbers 1988). With improved methodology, cross-peaks arising from intermolecular NOEs with at least three of the four crystallographically localized (Wlodawer *et al.* 1984) internal water molecules in BPTI were observed (Otting & Wüthrich 1989), thus providing a lower bound of 300 ps for the residence times of these buried water molecules. A subsequent ^{17}O MRD study (Denisov *et al.* 1996) demonstrated that the actual residence time of the most long-lived of these internal water molecules is actually seven orders of magnitude longer than the NOE-derived lower bound. Water cross-peaks, albeit of much lower intensity than for internal water molecules, have also been reported with fully solvent-exposed protein protons. For example, some 40 cross-peaks with solvent-exposed BPTI protons have been reported and used to draw conclusions about water residence times in the hydration layer (Otting *et al.* 1991*a*,*b*; Brunne *et al.* 1993). However, as discussed in § 5b, it now appears that all NOE-based inferences about protein surface hydration need to be thoroughly revised (Halle 2003; Modig *et al.* 2004).

(a) *Magnetic relaxation dispersion*

As one of the few methods that selectively probes water molecules in aqueous protein solutions, MRD of the quadrupolar ^{17}O water nucleus (Halle *et al.* 1999; Halle & Denisov 2001) has been used extensively to study both the internal and surface hydration of native (Denisov & Halle 1996; Halle 1998; Modig *et al.* 2004) and non-native (Halle *et al.* 2004) proteins in solution. MRD investigations of protein hydration usually entail measurements of the longitudinal relaxation rate, R_1, for the ^{2}H and/or ^{17}O isotopes in a protein solution made with isotope-enriched water. These R_1 measurements are performed as a function of the resonance frequency, ν_0, determined by the strength of the applied static magnetic field. A dataset, $R_1(\nu_0)$, covering two or more frequency decades is referred to as a dispersion profile. Depending on the circumstances, the MRD profile can provide quantitative information about several aspects of protein hydration, in particular about the number and residence times of long-lived (usually internal) water molecules and the mean rotational correlation time of water molecules at the protein surface.

In the MRD context, 'long-lived' association usually means a residence time longer than 1 ns. The origin of this operational definition is that a correlation time of 1 ns produces a dispersion centred at *ca.* 100 MHz, which is the highest ^{2}H or ^{17}O resonance frequency achievable with present-day superconducting NMR magnets. Fortuitously, this also happens to be a convenient borderline between internal water molecules, which usually have residence times in the range of 10^{-8} s to 10^{-4} s at room temperature, and water molecules interacting with the external protein surface, the vast majority of which have residence times in the range of 10^{-11} s to 10^{-10} s at room temperature (Denisov & Halle 1996; Halle 1998; Modig *et al.* 2004).

The relaxation dispersion, $R_1(\omega_0)$, of the quadrupolar water nuclei ^{2}H and ^{17}O is usually expressed in the form (Halle *et al.* 1999; Halle & Denisov 2001)

$$R_1(\omega_0) = R_{\mathrm{bulk}} + 0.2\mathcal{J}_{\mathrm{Q}}(\omega_0) + 0.8\mathcal{J}_{\mathrm{Q}}(2\omega_0), \qquad (5.1)$$

where R_{bulk} is the frequency-independent relaxation rate of the bulk solvent, measured separately on a reference sample, and $\omega_0 = 2\pi\nu_0$ is the ^{2}H or ^{17}O resonance frequency in angular frequency units. Molecular-level information about hydration is contained in the frequency-dependent quadrupolar spectral density, $\mathcal{J}_{\mathrm{Q}}(\omega_0)$. In the simplest case, the observed frequency dependence of R_1

within the experimentally accessible frequency window, typically 1–100 MHz, can be described by a single Lorentzian dispersion step. The spectral density function is then of the form

$$\mathcal{J}_{\mathrm{Q}}(\omega) = \alpha + \beta \frac{\tau_\beta}{1 + (\omega\tau_\beta)^2}. \tag{5.2}$$

Sometimes, a second dispersion step is indicated at higher frequencies than the β dispersion. This so-called γ dispersion is described by a term like the β term in equation (5.2).

The model used to extract molecular-level information from the amplitude parameters α and β, and the correlation time τ_β, recognizes two classes of hydration water, both of which exchange rapidly (see below) with bulk water. N_{hyd} water molecules have rotational correlation times that are significantly longer than in bulk water, but shorter than 1 ns. The effect of this class of perturbed water molecules is to increase the relaxation rate, R_1, above the bulk water value, R_{bulk}, without producing a frequency dependence (dispersion) in R_1 within the experimentally accessible range (less than 100 MHz). This is described by the parameter α, which may be expressed as (Halle *et al.* 1999; Halle & Denisov 2001)

$$\alpha = \frac{R_{\mathrm{bulk}}}{N_{\mathrm{T}}} N_{\mathrm{hyd}} \left(\frac{\langle \tau_{\mathrm{hyd}} \rangle}{\tau_{\mathrm{bulk}}} - 1 \right), \tag{5.3}$$

where N_{T} is the known water-to-protein mole ratio. For most proteins, the α contribution is produced by water molecules interacting with the external protein surface, and $\langle \tau_{\mathrm{hyd}} \rangle$ is the mean rotational correlation time for those water molecules.

For small solutes, the α term fully accounts for the hydration effect on R_1. Proteins, however, usually contain a small number, N_β, of water molecules with sufficiently long (greater than 1 ns) correlation times, τ_β, to produce an observable frequency dependence in R_1. These few water molecules are responsible for the dispersive β term in equation (5.2), with (Halle *et al.* 1999; Halle & Denisov 2001)

$$\beta = \frac{\omega_{\mathrm{Q}}^2}{N_{\mathrm{T}}} N_\beta S_\beta^2, \tag{5.4}$$

where ω_{Q} is the known rigid-lattice quadrupole coupling frequency. Numerous MRD studies have shown that only water molecules buried in internal cavities or in deep surface pockets have correlation times exceeding 1 ns at room temperature. Such internal water molecules tend to be extensively hydrogen-bonded to the protein and their highly restricted rotational motions give rise to an orientational order parameter, S_β, that is usually not far below the rigid-binding limit of unity.

Whereas X-ray diffraction probes *generic* spatial correlations, magnetic relaxation monitors *specific* temporal (and sometimes also spatial) correlations. In other words, magnetic relaxation experiments provide information about single-molecule dynamics, in particular, water rotation. Crudely speaking, a water molecule can either rotate in a given location or it can move to another place where it may rotate more rapidly. The correlation time τ_β may reflect either of these processes. Internal water molecules in small cavities do not usually rotate (except for librational motions) with respect to the protein, but undergo rotational diffusion together with the entire protein with rotational correlation time, τ_{R}. However, the effective rate of water rotation will be enhanced if the water molecule can escape into the bulk solvent, where its rotational correlation time is three to four orders of magnitude faster. The observed correlation time is dominated by the faster of these processes, according to

$$\frac{1}{\tau_\beta} = \frac{1}{\tau_{\mathrm{W}}} + \frac{1}{\tau_{\mathrm{R}}}, \tag{5.5}$$

where τ_{W} is the mean residence time in the internal hydration site.

At normal temperatures, the MRD experiment cannot monitor individual water molecules at the protein surface (as opposed to internal water molecules), but yields an average over all water molecules interacting with the protein surface. Because the dynamic perturbation of the solvent is short-ranged, only solvent molecules in direct interaction with the protein surface are significantly perturbed (Abseher *et al.* 1996; Halle 1998; Makarov *et al.* 2000; Marchi *et al.* 2002). The quantity $\langle \tau_{\mathrm{hyd}} \rangle$ can therefore be interpreted as the mean rotational correlation time for solvent molecules in direct contact with the protein surface. Technically, $\langle \tau_{\mathrm{hyd}} \rangle$ is the integral of the time-correlation function for the second-rank Legendre polynomial (Halle *et al.* 1999). However, the ratio $\langle \tau_{\mathrm{hyd}} \rangle / \tau_{\mathrm{bulk}}$, known as the rotational retardation factor, is independent of the rank and can be compared directly with results obtained by other methods. The number N_{hyd} can be estimated by dividing the water-accessible surface area of the protein, A_{P}, usually computed with a spherical probe of radius 1.4 Å, by the mean area, a_{W}, occupied by a water molecule at the surface. Geometric considerations suggest that a_{W} is close to 15 Å^2, in which case $N_{\mathrm{hyd}} \approx 500$ for a 15 kDa protein. Without specifying a_{W}, we can obtain the quantity $(\langle \tau_{\mathrm{hyd}} \rangle / \tau_{\mathrm{bulk}} - 1)/a_{\mathrm{W}}$ from the experimentally determined α parameter and the calculated surface area, A_{P}.

Figure 2 shows the distribution of $(\langle \tau_{\mathrm{hyd}} \rangle / \tau_{\mathrm{bulk}} - 1)/a_{\mathrm{W}}$ values derived from ^{17}O MRD profiles of 11 different monomeric globular proteins at 300 K. Each of the values included in figure 2*a* was determined from a fit of equations (5.1) and (5.2) (or its bi-Lorentzian extension, if motivated by a statistical *F*-test) to the MRD data. (A bi-Lorentzian dispersion shape can usually be attributed to internal water exchange in the nanosecond range or to protein self-association.) Water ^{17}O MRD profiles have also been obtained for several proteins with large water-filled cavities. These data are not included here because nanosecond water exchange among hydration sites within the cavity gives rise to a high-frequency dispersion, which is only partly sampled and therefore cannot be separated from the high-frequency plateau produced by the surface waters (Modig *et al.* 2003). Because the α-values derived from fits depend to some extent on the model adopted (one or two Lorentzians), we also show in figure 2*b*, model-independent upper bounds on $(\langle \tau_{\mathrm{hyd}} \rangle / \tau_{\mathrm{bulk}} - 1)/a_{\mathrm{W}}$ derived from the R_1 value measured at the highest investigated frequency (41–81 MHz). The mean and s.d. of $(\langle \tau_{\mathrm{hyd}} \rangle / \tau_{\mathrm{bulk}} - 1)/a_{\mathrm{W}}$ is 0.30 ± 0.04 Å^{-2} from fits and 0.35 ± 0.06 Å^{-2} from the highest frequency. In the following discussion, we use the former value.

For $a_{\mathrm{W}} = 15$ Å^2, we obtain a rotational retardation factor of $\langle \tau_{\mathrm{hyd}} \rangle / \tau_{\mathrm{bulk}} = 5.4 \pm 0.6$ for the 11 proteins. This is a

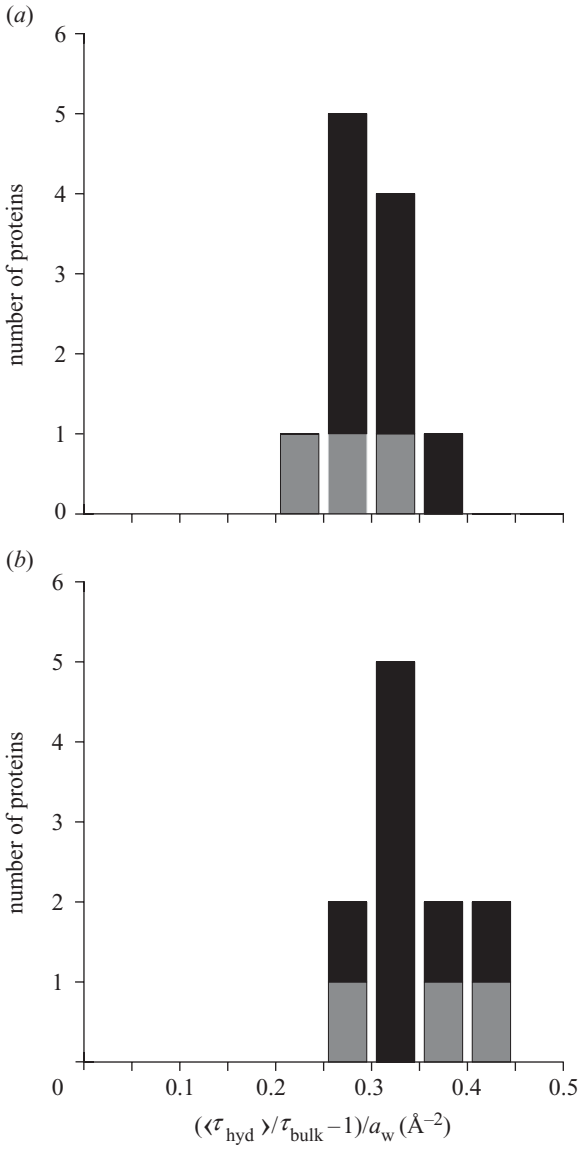

Figure 2. Mean rotational retardation of water molecules in the hydration layer of 11 monomeric globular proteins, deduced from ^{17}O MRD data at 300 K. (*a*) Results derived from the α parameter in the dispersion profile fit. (*b*) Upper bound derived from the R_1 value at the highest frequency: 41–49 MHz (grey) or 68–81 MHz (black).

significantly stronger rotational retardation than for free amino acids and other small organic molecules, for which $\langle\tau_{hyd}\rangle/\tau_{bulk}$ is usually in the range of 1.0–2.5 at room temperature (Halle 1998; Modig *et al.* 2004). This difference has been attributed to the presence of strongly motionally retarded water molecules at special locations on protein surfaces (Denisov & Halle 1996; Halle 1998; Modig *et al.* 2004). Even a few water molecules with correlation times in the range of 0.1–1 ns (at room temperature) could introduce a strong bias in the observed average correlation time $\langle\tau_{hyd}\rangle$. This interpretation is supported by recent molecular dynamics simulations, showing that the rotational correlation time (Marchi *et al.* 2002) and residence time (Henchman & McCammon 2002) distributions exhibit extended power-law tails.

An indication about the nature of these special hydration sites is obtained by examining the variation of $(\langle\tau_{hyd}\rangle/\tau_{bulk} - 1)/a_W$ among the 11 proteins. No significant correlation is found between this quantity and the net protein charge, the total number of charged groups, the total number of carboxylate groups, or any of these parameters divided by A_P. This finding is not unexpected because water–protein interactions are not significantly stronger than water–water interactions. Instead, the critical variable appears to be the surface topography (Denisov & Halle 1996; Halle 1998; Modig *et al.* 2004). Water molecules located in surface depressions experience geometric constraints that prevent the cooperative motions responsible for the fast rotational and translational dynamics in bulk water (see § 3). This MRD-derived picture of protein hydration dynamics is supported by several recent simulation studies that have confirmed the importance of surface topography and have failed to establish a correlation between water residence times and the chemical structure, charge or polarity of the contacting groups (Kovacs *et al.* 1997; Luise *et al.* 2000; Makarov *et al.* 2000; Henchman & McCammon 2002).

More detailed information about strongly perturbed surface water molecules has recently come from ^{2}H and ^{17}O MRD measurements at low temperatures (Modig *et al.* 2004). At room temperature, all water molecules at the protein surface, with the possible exception of a few deep and narrow surface pockets, have correlation times shorter than 1 ns and are therefore not resolved in the MRD profile. However, by lowering the temperature, the correlation times (0.1–1 ns at room temperature) of the most strongly perturbed water molecules can be made sufficiently long (greater than 1 ns) to allow direct observation of the dispersion associated with water exchange. MRD profiles were thus recorded for solutions of the protein BPTI in emulsified solutions down to 243 K (Modig *et al.* 2004). The ^{2}H MRD profile at 243 K (see figure 3) yields a correlation time, $\tau_\beta = 11 \pm 1$ ns, much shorter than the 70 ns rotational correlation time of the protein at this temperature. Because the four internal water molecules of BPTI exchange too slowly at 243 K to contribute to the measured ^{2}H relaxation rate, the observed dispersion must be a result of water molecules at the surface with a residence time in the range of 10–15 ns. The dispersion amplitude yields $N_\beta S_\beta^2 = 3.3 \pm 0.4$, implying that there are at least three such water molecules.

The high-frequency limit of the dispersion profile in figure 3 yields $\langle\tau_{hyd}\rangle/\tau_{bulk} = 2.1 \pm 0.2$ at 243 K for the remaining (*ca.* 265) water molecules in the hydration layer. This result is hardly compatible with the existence of extensive hydrogen-bond networks of fused water polygons, as inferred from cryocrystallographic studies of several proteins (Nakasako 1999; Esposito *et al.* 2000; Teeter *et al.* 2001). As discussed in § 4, these networks are likely to be cryo-artefacts, formed when water motions are quenched at *ca.* 200 K (Halle 2004). The experimental $\langle\tau_{hyd}\rangle/\tau_{bulk}$ value of 2.1 at 243 K is comparable to what has been obtained for small organic molecules at room temperature. However, ^{17}O relaxation studies of small-molecule hydration show that $\langle\tau_{hyd}\rangle$ has a significantly larger activation enthalpy than τ_{bulk}. Extrapolating these data down to 243 K, we find $\langle\tau_{hyd}\rangle/\tau_{bulk}$ values of 3.5, 9, 14 and 6 for methanol, propanol, *t*-butanol and benzene, respectively (Modig *et al.* 2004). The usual explanation of this phenomenon is that a clathrate-like hydration shell forms around such non-polar solutes, with water–water

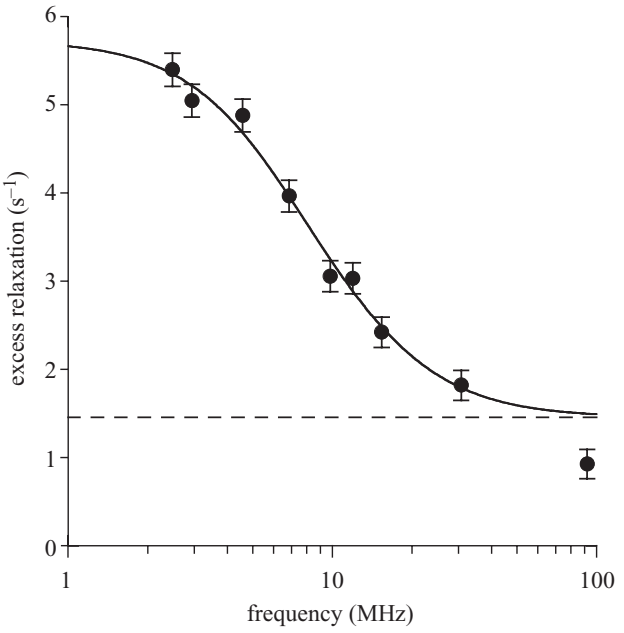

Figure 3. Water ^{2}H excess relaxation rate, $R_1 - R_{\mathrm{bulk}}$, versus resonance frequency for an emulsified aqueous solution of 8 mM BPTI at 243 K (Modig *et al.* 2004). The curve is a Lorentzian fit (omitting the highest-frequency point) and the dashed line corresponds to α.

hydrogen bonds that are considerably more long-lived than in bulk water because of the inability of the apolar (part of the) solute to participate in the fluctuating hydrogen-bond network.

In contrast to these small solutes, the low-temperature MRD results for BPTI show that $\langle\tau_{\mathrm{hyd}}\rangle/\tau_{\mathrm{bulk}}$ decreases at lower temperatures. This decrease was rationalized in terms of a few strongly perturbed water molecules that give rise to an observable dispersion at low temperatures and therefore no longer contribute to the α parameter. The remaining high-frequency excess relaxation rate is not compatible with a strong temperature dependence of the kind seen for small non-polar solutes. Consequently, clathrate-like hydration structures do not appear to be prevalent at the surface of BPTI. This is understandable, because few side-chains protrude from the surface to the extent that they are surrounded by a clathrate cage as for a small solute. Computer simulations also indicate that classical clathrate structures do not form at planar or concave hydrophobic patches on protein surfaces (Cheng & Rossky 1998). For BPTI, and for most other native globular proteins (Harpaz *et al.* 1994; Murphy *et al.* 1998), *ca.* 60% of the solvent-accessible surface area is contributed by non-polar atoms. The inferred absence of classical hydrophobic hydration structures at the surface of BPTI, which would have caused $\langle\tau_{\mathrm{hyd}}\rangle/\tau_{\mathrm{bulk}}$ to increase strongly at lower temperatures, suggests that the entropic penalty for the residual exposure of non-polar groups at the surface of the native protein is smaller than expected on the basis of small-molecule solvation thermodynamics (for the same overall non-polar surface area). If this is true, hydrophobic side-chains stabilize native protein structures not only through burial in the protein core, but also, albeit to a lesser extent, when partly exposed at the protein surface.

(b) *Intermolecular nuclear Overhauser effect*

Information about protein hydration dynamics has also been derived from intermolecular ^{1}H–^{1}H NOEs between water and protein protons (Otting & Liepinsh 1995; Otting 1997). In most such studies, the experimental observable is the ratio of cross-peak intensities in NOESY and ROESY spectra. Provided sufficiently short mixing times are used, this can be translated into the ratio $\sigma_{\mathrm{L}}/\sigma_{\mathrm{R}}$ of the laboratory-frame (σ_{L}) and rotating-frame (σ_{R}) cross-relaxation rates. These are governed by the dipolar spectral density function, $\mathcal{J}_{\mathrm{D}}(\omega)$ according to (Neuhaus & Williamson 2000)

$$\sigma_{\mathrm{L}}(\omega_0) = 0.6\mathcal{J}_{\mathrm{D}}(2\omega_0) - 0.1\mathcal{J}_{\mathrm{D}}(0), \tag{5.6a}$$

$$\sigma_{\mathrm{R}}(\omega_0) = 0.3\mathcal{J}_{\mathrm{D}}(\omega_0) + 0.2\mathcal{J}_{\mathrm{D}}(0). \tag{5.6b}$$

Because $\mathcal{J}_{\mathrm{D}}(\omega)$ is a monotonically decreasing function, it follows that the ratio $\sigma_{\mathrm{L}}/\sigma_{\mathrm{R}}$ can vary from $+1$ to -0.5. The limit $\sigma_{\mathrm{L}}/\sigma_{\mathrm{R}} = 1$ corresponds to fast dynamics with $\mathcal{J}_{\mathrm{D}}(0) = \mathcal{J}_{\mathrm{D}}(\omega_0) = \mathcal{J}_{\mathrm{D}}(2\omega_0)$, whereas the limit $\sigma_{\mathrm{L}}/\sigma_{\mathrm{R}} = -0.5$ corresponds to slow dynamics with $\mathcal{J}_{\mathrm{D}}(0) \gg \mathcal{J}_{\mathrm{D}}(\omega_0) > \mathcal{J}_{\mathrm{D}}(2\omega_0)$. Here, 'fast' and 'slow' should be understood in relation to $1/\omega_0 \approx 300$ ps (for a ^{1}H resonance frequency of 600 MHz).

NOE data acquired at a single frequency are not as readily interpreted as MRD data spanning a wide frequency range. In particular, the separation of the strength of the dipole–dipole couplings, depending on the number of interacting water protons and their distances from a particular protein proton, from the rate of modulation of the dipole–dipole vectors, containing the desired information about hydration dynamics, is highly model dependent (Ayant *et al.* 1977; Brüschweiler & Wright 1994; Otting 1997). For a pair of protons at fixed separation, r_{HH}, rigidly attached to a protein that tumbles isotropically with rotational correlation time, τ_{R}, the dipolar spectral density function is of the form (Abragam 1961)

$$\mathcal{J}_{\mathrm{D}}(\omega) = \frac{K}{r_{\mathrm{HH}}^6}\,\frac{\tau_{\mathrm{R}}}{1 + (\omega\tau_{\mathrm{R}})^2}, \tag{5.7}$$

where $K = [(\mu_0/4\pi)\ \hbar\ \gamma^2]^2 = 5.695 \times 10^{11}$ Å^6 s^{-2}. An expression like this, but with τ_{R} replaced by an effective correlation time as in equation (5.5), may be a reasonable approximation for NOEs with long-lived water molecules trapped in cavities or deep crevices (Denisov *et al.* 1997*b*).

When applied to surface hydration, the intramolecular spectral density in equation (5.7) has two major shortcomings: it takes into account only a single pair of protons and it neglects their relative translational motion. Because only one water ^{1}H resonance is observed, the measured cross-relaxation rates are, in principle, affected by dipole–dipole couplings between a particular protein proton and all water protons in the sample. Although the square of the dipole–dipole coupling falls off with distance as r^{-6} (as in equation (5.7)), the number of water protons at a given distance increases as r^2 and the characteristic time for angular modulation of the proton–proton vector by water translational diffusion also increases as r^2. On integrating the resulting r^{-2} dependent product of these factors from $r = d$ (the distance of closest approach) to infinity, one recovers the well-known $1/d$ scaling of $\mathcal{J}_{\mathrm{D}}(0)$ (Abragam 1961). Because the contribution from solvent protons at

separation r falls off as r^{-2} (rather than r^{-6}), the cross-relaxation between protein and water protons does not, in general, reflect local hydration dynamics, but is dominated by long-range dipole–dipole couplings with bulk water (Halle 2003).

In studies of protein hydration, water–protein NOEs have been interpreted either with the intramolecular spectral density in equation (5.7) (or a variant that takes internal motions into account), or with an intermolecular spectral density based on a model where the dipole-coupled water and protein protons reside in spherical particles undergoing translational and rotational diffusion (Ayant *et al.* 1977). If the water protons are placed at the centre of the water sphere, which is an excellent approximation owing to the fast water rotation, water dynamics enters the model solely via the water translational diffusion coefficient D. For given values of the other model parameters, a measured σ_L/σ_R ratio can thus be transformed into a water diffusion coefficient (Otting *et al.* 1991*a*; Otting & Liepinsh 1995; Otting 1997). In NOE studies of protein hydration, it has invariably been assumed (explicitly or implicitly) that the cross-relaxation rates involve only one or a few water molecules in the immediate vicinity of the observed protein proton. However, if the cross-relaxation rates are dominated by long-range dipole–dipole couplings, the diffusion coefficient D, deduced from the model, mainly reflects the dynamics of bulk water.

To characterize the perturbation of water dynamics by the protein, i.e. the hydration dynamics, a more general model is needed that allows the water diffusion coefficient to take different values in the hydration layer (D_{hyd}) and in the bulk solvent (D_{bulk}). An analytical spectral density function for such a non-uniform diffusion model has recently been derived (Halle 2003). The model describes the protein as a sphere covered by a hydration layer with a reduced water diffusion coefficient D_{hyd}. The thickness of this hydration layer is determined by the condition that the volume of the spherical shell equals the volume occupied by a monolayer of N_{hyd} water molecules on the real (non-spherical) protein surface. Because water translation and rotation are both rate-limited by hydrogen-bond dynamics (Halle 1998; Marchi *et al.* 2002; Geiger *et al.* 2003), the translational retardation factor D_{bulk}/D_{hyd} that enters the non-uniform diffusion model can be set equal to the rotational retardation factor $\langle\tau_{hyd}\rangle/\tau_{bulk}$ deduced from MRD data. The non-uniform diffusion model therefore allows NOE and MRD data to be interpreted within the same theoretical framework.

The most extensive NOE study of surface hydration has been performed on the protein BPTI at 277 K: 44 protein–water cross-peaks were reported, all with positive σ_L values (Otting *et al.* 1991*a*,*b*; Brunne *et al.* 1993). For half of these cross-peaks, the standard interpretation of the experimental σ_L/σ_R ratios suggests water residence times in the range of 100–500 ps (Brunne *et al.* 1993), much longer than found by MRD (Modig *et al.* 2004). As positive σ_L rates are invariably small, the corresponding cross-peaks are highly susceptible to competing magnetization transfer pathways, in particular exchange-relayed NOEs involving labile BPTI protons. Calculations with the non-uniform diffusion model indicate that a labile proton at a distance of 6 Å can affect both σ_L and σ_R rates significantly. In the crystal structure 5PTI (Wlodawer *et al.* 1984), 83% of the non-labile BPTI protons are within 6 Å of a labile proton or a proton in one of the four internal water molecules (see figure 4). Similar results are obtained for other proteins. A reanalysis of the NOE data for BPTI leads to the following conclusions (Modig *et al.* 2004).

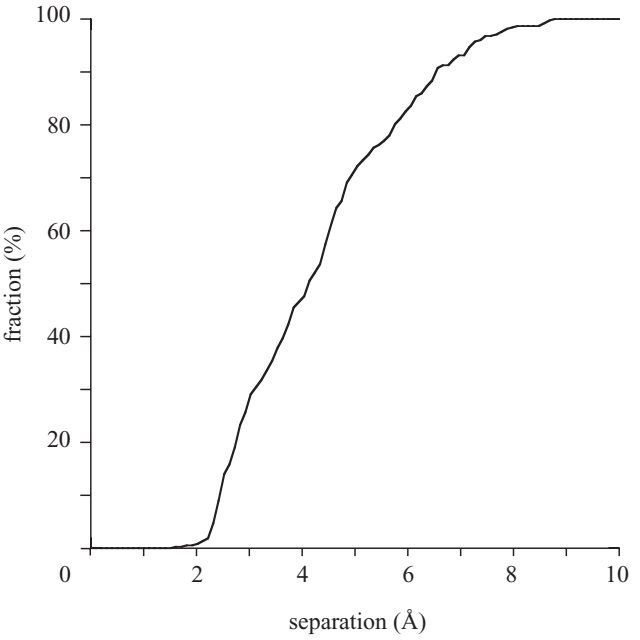

Figure 4. The fraction non-labile protons in BPTI that have at least one labile BPTI proton or internal water proton within the indicated distance. The calculation is based on the crystal structure 5PTI (Wlodawer *et al.* 1984) with four internal water molecules.

(i) The observed variation in the σ_L/σ_R ratio among different protons on the surface of BPTI is mainly caused by variations in proton burial depth or solvent accessibility, rather than by variations in hydration water dynamics.
(ii) The NOE method is insensitive to water dynamics in the hydration layer. In fact, under the conditions of the BPTI study, the σ_L/σ_R ratio cannot distinguish between a 10-fold dynamic retardation and no retardation at all (see figure 5).
(iii) Under the conditions of the BPTI study, the dominant bulk water contribution rules out σ_L/σ_R values significantly larger than 0.5. A ratio of 1.0, as reported for 10 out of the 44 cross-peaks, therefore indicates that the measured cross-peak intensities do not faithfully report on the cross-relaxation rates.

A similar re-examination of NOE data for the cyclic nonapeptide oxytocin (Otting *et al.* 1991*a*, 1992; Modig *et al.* 2004) shows that the sign reversal observed for water–peptide NOEs at subzero temperatures can be explained by the reduced diffusion coefficient of bulk water. A negative NOE should therefore not be taken as evidence for substantially prolonged residence times of hydration water. Individual hydration water molecules can dominate the NOE only if they are located near the observed solute proton and if their mobility is very much reduced compared with bulk water. This is the case for water molecules

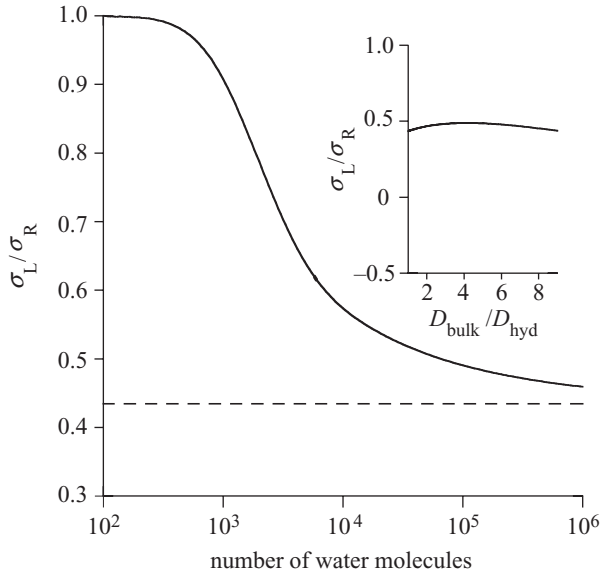

Figure 5. Ratio of water–BPTI cross-relaxation rates in the laboratory (σ_L) and rotating (σ_R) frames at 500 MHz ^{1}H NMR frequency, predicted by the non-uniform diffusion model (Halle 2003). The main plot shows the slow convergence of σ_L/σ_R as dipole couplings to water molecules in successive layers are included. The insert shows that the ratio σ_L/σ_R is nearly independent of the water diffusion coefficient, D_{hyd}, in the hydration layer. The protein was modelled as a sphere of radius 15 Å, with a 2.5 Å distance of closest approach between BPTI and water protons. The thickness of the hydration layer is 2.4 Å, corresponding to $N_{hyd} = 268$. The rotational correlation time of BPTI is 6.7 ns and the bulk water diffusion coefficient is 1.2×10^{-9} $m^2\,s^{-1}$, both pertaining to 277 K. For the main plot, the translational retardation factor $D_{bulk}/D_{hyd} = 2$, in accordance with MRD results for BPTI.

trapped in cavities inside proteins, like the four internal water molecules in BPTI (Otting & Wüthrich 1989). In such cases, water–protein NOEs can be interpreted in terms of an intramolecular spectral density function (equations (5.5) and (5.7)), where the strong distance dependence (r_{HH}^{-6}) provides a geometric constraint on the location of long-lived water molecules.

6. OTHER SPECTROSCOPIC PROBES OF HYDRATION DYNAMICS

(a) *Dielectric relaxation spectroscopy*

DRS was among the first methods used to probe the dynamics of protein solutions, pre-dating the modern view of protein structure (Oncley 1938). Some of the early DRS studies were taken to support the popular, but incorrect, picture of an ice-like hydration layer (Grant 1965). DRS has a superficial resemblance to MRD, but there are fundamental differences (Fröhlich 1958; Abragam 1961; Böttcher *et al.* 1973). The dielectric dispersion profile, that is, the frequency dependence of the real part of the complex relative permittivity, is usually represented as a sum of Lorentzian (Debye-type) dispersion terms,

$$\varepsilon'(\omega) = \varepsilon_\infty + \sum_k \frac{a_k}{1 + (\omega\tau_k)^2}\,, \qquad (6.1)$$

where τ_k is the dielectric relaxation time of the kth dispersion and a_k is the corresponding contribution to the zero-frequency permittivity (the usual dielectric constant). The permittivity measured at optical frequencies, ε_∞, represents electronic polarizability. On comparing equation (6.1) with equations (5.1) and (5.2), we note two fundamental differences. Because the correlation time, τ_β, appears in the numerator of the spectral density in equation (5.2), even a single water molecule can have a large effect on the MRD profile if it rotates much more slowly than in bulk water. This is the case for most internal water molecules. In DRS, water molecules contribute to the amplitudes a_k in proportion to their numbers (as in MRD), but independently of their dynamics. This makes DRS a much less sensitive probe of rotationally retarded water molecules. Internal water molecules therefore cannot be detected by DRS. By accessing the giga- to terahertz frequency range, DRS can, in principle, observe hydration water dynamics directly. In dilute protein solutions, however, this advantage is largely offset by the low sensitivity. The second fundamental difference between DRS and MRD is related to the interactions used to probe the system. Whereas ^{17}O MRD uses weak, non-perturbing nuclear interactions to selectively monitor water molecules, DRS involves all degrees of freedom that respond to the applied oscillating electric field. This includes not only water rotation, but also protein tumbling and various motions of counterions and charged or dipolar side-chains at the protein surface. Moreover, whereas MRD probes single-molecule dynamics, DRS measures the collective response of the entire system, comprising many degrees of freedom, some of which are strongly coupled. In contrast to MRD, the interpretation of the amplitude factors a_k in equation (6.1) is therefore highly non-trivial.

The dielectric dispersion profile from a dilute protein solution is dominated by two dispersion steps (see figure 6): the β dispersion near 10 MHz, which reflects protein tumbling, and the γ dispersion near 20 GHz, caused by (collective) reorientation in bulk water. In addition, a small dispersion step is usually seen near 100 MHz, corresponding to $\tau_\delta \approx 1$ ns. The origin of this δ dispersion is controversial, but most authors attribute it, at least partly, to water rotation in the hydration layer (Dachwitz *et al.* 1989; Pethig 1992, 1995; Knocks & Weingärtner 2001). To be observable against the background of bulk water (some 10^4 bulk water molecules at a protein concentration of 5 mM), the δ dispersion must then be attributed to a large number of hydration water molecules (in the order of 10^2). Many DRS studies have thus concluded that a sizeable fraction (typically, about one-half) of the water molecules in the hydration layer are strongly rotationally retarded, with $\langle\tau_{hyd}\rangle/\tau_{bulk}$ in the range of 10^2–10^3 (Dachwitz *et al.* 1989; Pethig 1992, 1995; Miura *et al.* 1994; Wei *et al.* 1994). This conclusion is grossly inconsistent with the MRD results (see § 5a), yielding $\langle\tau_{hyd}\rangle/\tau_{bulk} \approx 2$ for the vast majority of water molecules in the hydration layer. (The few more strongly rotationally retarded water molecules that increase the global average $\langle\tau_{hyd}\rangle/\tau_{bulk}$ to about 5 will not make a significant contribution to the dielectric dispersion profile.) We must therefore conclude that the δ dispersion is not a result of water dynamics at all. As seen from figure 6, the hydration contribution to the dielectric dispersion profile, expected for

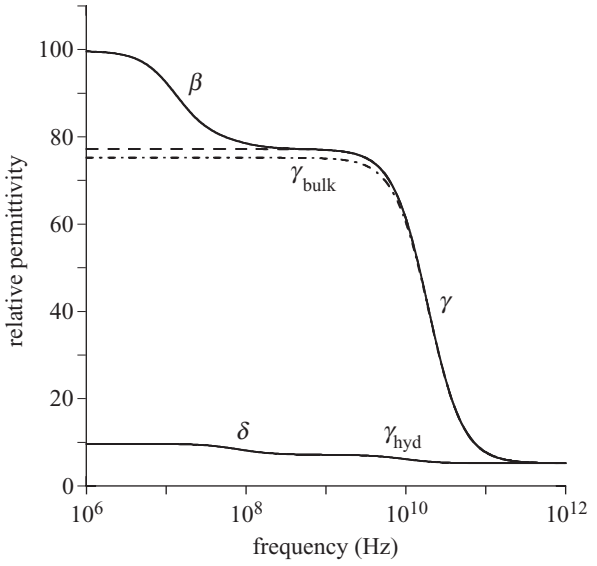

Figure 6. Frequency dependence of the real part, $\varepsilon'(\nu)$, of the complex relative permittivity of an aqueous protein solution at 298 K. The parameters of the β and δ dispersions were taken from experimental data for ubiquitin (Knocks & Weingärtner 2001), and were scaled to a protein concentration of 5 mM. The γ dispersion was decomposed into a bulk water part, with $\tau_{\mathrm{bulk}} = 8.3$ ps (Kaatze 1989), and a contribution from the hydration layer, with $\langle\tau_{\mathrm{hyd}}\rangle/\tau_{\mathrm{bulk}} = 2$ and $N_{\mathrm{hyd}} = 300$. The upper solid curve shows the total $\varepsilon'(\nu)$, while the lower solid curve shows the contributions from the δ and γ_{hyd} dispersions. The dashed curve corresponds to the total γ dispersion (bulk plus hydration water), whereas the dash–dot curve shows the bulk water contribution, γ_{bulk}.

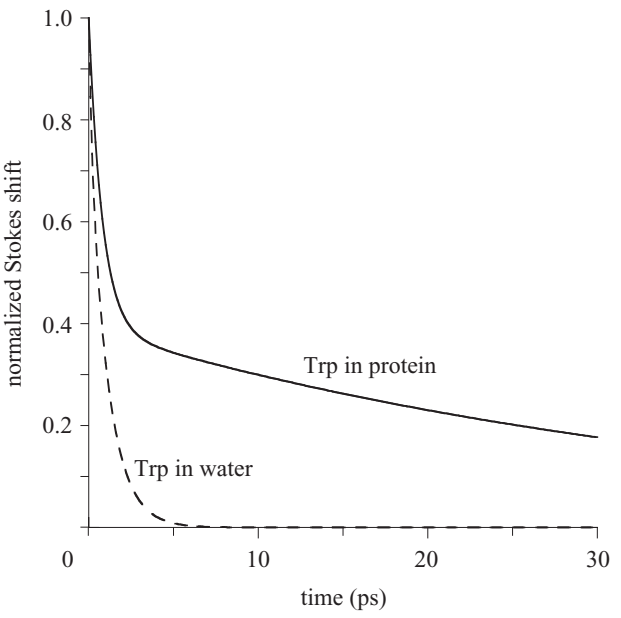

Figure 7. Normalized DSS, $S(t)$, for tryptophan (Trp) in bulk water (dashed line) and for Trp-113 in subtilisin *Carlsberg* (solid line). The bi-exponential curves are based on experimentally determined amplitudes and decay times (Pal *et al.* 2002*b*).

$\langle\tau_{\mathrm{hyd}}\rangle/\tau_{\mathrm{bulk}} = 2$ (from MRD) and $N_{\mathrm{hyd}} = 300$, is very small in amplitude (at a protein concentration of 5 mM) and overlaps with the bulk water dispersion.

To extract reliable information about protein hydration dynamics from DRS, very accurate measurements at relatively high protein concentrations would seem to be required (Oleinikova *et al.* 2004). In addition, a rigorous theory is needed to link observables to molecular model parameters. Computer simulations can provide valuable guidance in this regard (Boresch *et al.* 2000). A recently proposed microscopic theory of dielectric relaxation in protein solutions (Nandi & Bagchi 1997, 1998) does not appear to fulfil these needs (Boresch & Steinhauser 2001). This theory invokes the erroneous concept of an equilibrium between bound and free water (see § 2) and a rotation-exchange model that, although extensively used in NMR (Halle *et al.* 1999), does not seem to be useful in connection with dielectric relaxation, except in the presence of chemical processes (Schwarz 1967).

(b) *Time-resolved fluorescence spectroscopy*

A more recently developed experimental approach to protein hydration dynamics employs time-resolved fluorescence spectroscopy to monitor the time evolution of the frequency, $\nu(t)$, of the emission maximum after electronic excitation of an intrinsic tryptophan residue in the protein or a covalently attached extrinsic fluorophore (Pal *et al.* 2002*a*; Pal & Zewail 2004). The frequency shift caused by the difference in interactions with the environment between the ground and excited states, known as the Stokes shift, changes as the environment relaxes in response to the altered charge distribution produced by electronic excitation. This evolution is described by the normalized DSS,

$$S(t) = \frac{\nu(t) - \nu(\infty)}{\nu(0) - \nu(\infty)} \,. \tag{6.2}$$

If the excitation occurs without change in nuclear configuration, the measured quantity, $S(t)$, can be related to the similarly normalized difference, $\Delta E(t)$, in mean interaction energy of the excited and ground states. Accordingly, the evolution described by equation (6.2) is referred to as solvation dynamics. When the environment is heterogeneous, as for a tryptophan residue in a protein, 'solvation' must be understood in a generalized sense to include both protein and solvent degrees of freedom. The potential for confusion is even greater when the term 'solvation dynamics' is applied to the DSS method used to study the phenomenon (Nandi *et al.* 2000). The interpretation of DSS data relies on the linear response approximation (Fleming & Cho 1996): provided that the perturbation is sufficiently weak, the non-equilibrium response function, $S(t)$, can be identified with the time correlation function, $C(t) = [\langle\Delta E(0)\,\Delta E(t)\rangle - \langle\Delta E\rangle^2]/[\langle(\Delta E)^2\rangle - \langle\Delta E\rangle^2]$, which describes thermal fluctuations of $\Delta E(t)$ around its average, $\langle\Delta E\rangle$, when the environment is in equilibrium with respect to the (ground or excited state) charge distribution. The validity of the linear response approximation in DSS studies has recently been questioned (Bedard-Hearn *et al.* 2003).

Figure 7 shows DSS curves for tryptophan in water and in the protein subtilisin *Carlsberg* (Pal *et al.* 2002*b*). Similar results have been reported for other proteins (Pal *et al.* 2002*c*; Peon *et al.* 2002). For tryptophan in water, the DSS curve exhibits a sub-picosecond inertial decay, associated with water librations (Jimenez *et al.* 1994), followed by a diffusive decay with a time constant $\tau_{\mathrm{bulk}}^{\mathrm{DSS}} \approx 1$ ps

(Shen & Knutson 2001; Pal *et al.* 2002*b*). For the single tryptophan residue in subtilisin *Carlsberg*, 60% of the DSS decays on the same time-scale (0.8 ps) as $\tau_{\mathrm{bulk}}^{\mathrm{DSS}}$, whereas the remaining 40% of the shift has a much slower decay ($\tau_{\mathrm{solv}}^{\mathrm{DSS}} = 38$ ps). Zewail and coworkers attribute both of these decays to water dynamics in the hydration layer of the protein (Pal *et al.* 2002*a–c*; Peon *et al.* 2002; Pal & Zewail 2004). Specifically, they propose that the hydration layer is composed of 'free' and 'bound' water molecules. The essential difference between these putative categories is that 'free' water molecules undergo rotational diffusion as in bulk water while remaining inside the hydration layer, whereas 'bound' water molecules are rigidly attached to the protein during their residence time. Furthermore, they relate the short decay time (similar to $\tau_{\mathrm{bulk}}^{\mathrm{DSS}}$) to the dielectric relaxation time of 'free' (or bulk) water, while the long decay time, $\tau_{\mathrm{solv}}^{\mathrm{DSS}}$, is interpreted as the mean residence time of 'bound' water molecules. This interpretation, implying that hydration water is dynamically retarded by one to two orders of magnitude ($\tau_{\mathrm{solv}}^{\mathrm{DSS}}/\tau_{\mathrm{bulk}}^{\mathrm{DSS}} \approx 40$ for subtilisin *Carlsberg*), is clearly inconsistent with the MRD results ($\langle\tau_{\mathrm{hyd}}\rangle/\tau_{\mathrm{bulk}} \approx 2$).

The Zewail model is problematic in several respects. If the hydration layer consisted of 'free' and 'bound' water molecules, as postulated, then one would expect bimodal distributions of residence times and rotational correlation times for hydration water. However, all simulations show that these distributions are unimodal (Abseher *et al.* 1996; Luise *et al.* 2000; Makarov *et al.* 2000; Marchi *et al.* 2002; Henchman & McCammon 2002). Also, from a structural–energetic point of view, the notion of 'free' and 'bound' water molecules in the hydration layer is objectionable. Simulations show that all water molecules, whether in the hydration layer or in bulk water, have approximately the same number (3–4) of hydrogen bonds (Henchman & McCammon 2002). Furthermore, the 1 ps DSS decay can hardly be identified with the dielectric relaxation time, τ_{bulk}, of bulk water, which is 8.3 ps at 298 K (Kaatze 1989). The order-of-magnitude discrepancy between $\tau_{\mathrm{bulk}}^{\mathrm{DSS}}$ and τ_{bulk} is not unexpected; in a zeroth-order continuum model, the characteristic time for solvent relaxation in response to an instantaneously created dipole is $3\tau_{\mathrm{bulk}}/(2\varepsilon_0 + 1) \approx 0.2$ ps, where $\varepsilon_0 \approx 78$ is the dielectric constant of water (Papazyan & Maroncelli 1995).

Another serious concern is the unproven assertion that the slow DSS decay of a tryptophan residue in a protein is a manifestation of slow-water dynamics (Pal *et al.* 2002*a*; Pal & Zewail 2004). An inspection of the crystal structure (1SBC) of subtilisin *Carlsberg* shows that the Trp-133 side-chain is largely buried, with only one edge of the indole ring exposed to the solvent. There are 15 polar protein atoms within 5 Å of this side chain and the dipolar amide group of Asn-117 is in van der Waals contact with one face of the indole ring. The decay time, $\tau_{\mathrm{solv}}^{\mathrm{DSS}} = 38$ ps, may thus reflect internal motions in the protein in response to the excited-state charge distribution. This alternative interpretation is further supported by the finding that the fluorescence anisotropy decays with a time constant of 55 ps (Pal *et al.* 2002*b*). Because the DSS is affected by the motions of the indole (reflected in the anisotropy decay), as well as motions of the surrounding interacting polar and charged protein atoms (which are only partly correlated with indole motions), $\tau_{\mathrm{solv}}^{\mathrm{DSS}}$ is, indeed, expected to be somewhat shorter than 55 ps.

In the protein monellin, where $\tau_{\mathrm{solv}}^{\mathrm{DSS}} = 16$ ps was reported (Peon *et al.* 2002), one face of the indole ring in the examined Trp-3 side chain is solvent exposed, but there are six charged groups within 8 Å of this residue (in the crystal structure 4MON). A recent 2 ns molecular dynamics simulation of monellin in water, using an excited state charge distribution corresponding to a dipole moment of 5.7 D for the Trp-3 indole, shows that the energy correlation function $C(t)$ is dominated by intraprotein interactions, which decay on the time-scale of the experimental $\tau_{\mathrm{solv}}^{\mathrm{DSS}}$, whereas the smaller water contribution decays on a much shorter time-scale (L. Nilsson, unpublished results), as expected from the MRD results.

Although DSS studies with femtosecond resolution can potentially furnish valuable insights into fast water dynamics in proteins, the currently available results and their interpretation must be regarded with caution until the DSS curve has been unambiguously decomposed into protein and water contributions. The same caveat applies to DSS studies of hydration in other heterogeneous systems, such as micelles, microemulsions and membranes (Bhattacharyya & Bagchi 2000; Nandi *et al.* 2000). Slow DSS decays on the 0.1–1 ns time-scale, as well as DRS data, from such complex systems have been attributed to a slow component in hydration dynamics, purportedly a generic feature of 'constrained water' (Bhattacharyya & Bagchi 2000; Nandi *et al.* 2000). Contrary to the conclusion of these authors, such interpretations are decidedly inconsistent with the results of numerous NMR relaxation studies of biomolecular solutions and complex fluids of non-biological origin (Halle 1998). The notion of very slow hydration water dynamics has received apparent support from molecular dynamics simulations of surfactant micelles. In particular, the orientational time correlation function for water outside a disc-shaped micelle was found to exhibit a long-time tail with a decay time exceeding several 100 ps (Balasubramanian & Bagchi 2002; Pal *et al.* 2002*d*). This tail was attributed to 'bound' water molecules with long residence times at the micelle surface. An alternative explanation of the tail in the correlation function, which does not invoke long-lived water binding, presents itself once it is realized that the studied system is anisotropic on the time-scale of the simulation. The dipolar correlation function thus exhibits a tail associated with micelle tumbling on the nanosecond time-scale.

7. FROM WATER DYNAMICS TO HYDRODYNAMICS

Measurements of transport coefficients of proteins in solution, such as the rotational and translational diffusion coefficients, the sedimentation coefficient and the intrinsic viscosity, have long been used to estimate the amount of hydration water (Kuntz & Kauzmann 1974; Squire & Himmel 1979). This hydrodynamic approach to protein hydration is based on the idea that a certain amount of water at the protein surface, in some sense, migrates along with the protein and thus contributes to its effective hydrodynamic volume. The amount of hydration water is obtained from the difference between the hydrodynamic volume and the bare protein volume (obtained from the partial specific volume or from the crystal structure). This

operational definition of protein hydration has several deficiencies. To expose these, we consider the case of rotational diffusion.

The rotational motion of a protein molecule is at least three orders of magnitude slower than the relaxation of its angular momentum and can therefore be described accurately by a rotational diffusion equation. The dynamic protein–solvent coupling is embodied in Einstein's fluctuation–dissipation theorem, relating the rotational diffusion coefficient, D_R, to the rotational friction coefficient, ζ_R: $D_R = k_B T/\zeta_R$ (Zwanzig 2001). When this is combined with the result of macroscopic continuum hydrodynamics (Landau & Lifshitz 1959) for the friction coefficient of a sphere of radius a undergoing steady rotation in a solvent of shear viscosity η_0, one obtains the (rotational) Stokes–Einstein relation

$$D_R^{SE} = \frac{k_B T}{8\pi\eta_0 a^3}. \tag{7.1}$$

More elaborate expressions have been derived for ellipsoidal solutes (Perrin 1936). When applied to globular proteins, equation (7.1) overestimates the rotational diffusion coefficient by about a factor of 2. As an example, consider HEWL. Using either the crystal structure or the partial specific volume in solution, one obtains a molecular volume of 16 nm^3. Inserted into equation (7.1), this yields $D_R = 42\ \mu s^{-1}$ in H_2O at 20 °C. If the somewhat elongated shape of HEWL is modelled by a prolate spheroid of aspect ratio 1.5, D_R is reduced to 40 μs^{-1}, still a factor of 2 above the experimental value of $20 \pm 1\ \mu s^{-1}$ (Buck *et al.* 1995). Whereas early workers attributed such discrepancies to 'bound' water migrating with the protein, hydration effects turn out to be less important than large-scale shape irregularities, such as the binding cleft in HEWL, which make the rotating protein displace a larger amount of solvent than would a compact protein of the same volume (Halle & Davidovic 2003).

In recent years, efficient numerical methods have been developed for computing the hydrodynamic friction tensors of rigid biomolecular structures described in atomic detail (Garcia de la Torre & Bloomfield 1981; Garcia de la Torre *et al.* 2000; Zhao & Pearlstein 2002). Such detailed modelling of protein shape brings theory much closer to experiment and also removes most of the variation in apparent hydration among different proteins. Nevertheless, even molecular hydrodynamics does not quite bridge the gap between theory and experiment. Typically, the rotational diffusion coefficient is still 30% too large. This discrepancy, which exceeds the experimental uncertainty in D_R by an order of magnitude, is usually ascribed to about half a monolayer of 'tightly bound' water molecules (Venable & Pastor 1988; Byron 1997; Garcia de la Torre 2001; Korzhnev *et al.* 2001).

What are the implications of attributing the 30% discrepancy in D_R to 'tightly bound' water molecules? Because D_R is inversely proportional to volume (see equation (7.1)), the volume of this 'rigid' hydration shell is, in the case of HEWL, $0.30 \times 16 = 4.8$ nm^3. If a water molecule occupies 25 Å^3 at the protein surface, as suggested by Voronoi analysis of protein crystals (Gerstein & Chothia 1996), then this volume corresponds to *ca.* 200 water molecules. If these water molecules were immobilized at the protein surface, they would contribute to the hydrodynamic friction in the same way as protein atoms. According to conventional wisdom, this will still be the case if these water molecules exchange with bulk water, as long as their residence times are longer than the rotational correlation time of the protein so that they migrate with the rotating protein. This widely accepted interpretation thus implies that *ca.* 200 water molecules on the surface of HEWL have residence times longer than the (rank-2) rotational correlation time of HEWL, $\tau_R^{(2)} = (6D_R)^{-1} = 8$ ns. This interpretation is clearly incompatible with the picosecond dynamics in the hydration layer deduced from MRD experiments (see § 5a).

This paradox can be resolved by allowing the viscosity in the first hydration shell to differ from the bulk water viscosity (Halle & Davidovic 2003). By solving the hydrodynamic equations of motion and computing the frictional torque from the stress tensor (Landau & Lifshitz 1959; Wolynes 1980; Brilliantov & Krapivsky 1991), one finds for the rotational diffusion coefficient, D_R, of a spherical 'protein' of volume V_P, immersed in an incompressible solvent with viscosity η_{hyd} within a spherical shell of volume V_{hyd} and the bulk value η_{bulk} elsewhere:

$$\frac{D_R}{D_R^{SE}} = 1 - (1 - \alpha_R)\left(1 - \frac{\eta_{bulk}}{\eta_{hyd}}\right), \tag{7.2}$$

where $\alpha_R = V_P/(V_P + V_{hyd})$ and D_R^{SE}, as given by equation (7.1), is the rotational diffusion coefficient in the absence of hydration effects. This result has the expected limits. In the absence of hydration, meaning $\eta_{hyd} = \eta_{bulk}$ and/or $V_{hyd} = 0$, equation (7.2) reduces to $D_R = D_R^{SE}$. In the 'solvent-berg' limit, where $\eta_{hyd} \gg \eta_{bulk}$ so that a negligible fraction of the viscous energy dissipation occurs in the hydration shell, we also recover the Stokes–Einstein equation (7.1), but now with a hydrodynamic volume that includes the effectively rigid hydration shell.

Equation (7.2) should also be approximately valid for a real (non-spherical) protein if the left-hand side is replaced by D_R/D_R^0, the ratio of the rotational diffusion coefficient of the real protein in the real perturbed solvent (D_R) to that in an unperturbed bulk solvent (D_R^0). Furthermore, the variation of the local viscosity over the structurally and chemically heterogeneous protein surface can be taken into account by replacing η_{bulk}/η_{hyd} by the spatial average $\langle\eta_{bulk}/\eta_{hyd}\rangle$ over the hydration layer volume V_{hyd}. This η_{hyd}^{-1} averaging makes physical sense: even if η_{hyd} is very large in a small region, D_R should not be affected much because most of the viscous dissipation occurs outside this small region in any case. Finally, the local viscosity η_{hyd} is taken to be proportional to the water rotational correlation time, τ_{hyd}, as is the case for bulk water over a wide temperature range (Modig & Halle 2002). After these approximations, the hydration effect on the rotational diffusion coefficient of a protein can be expressed as (Halle & Davidovic 2003)

$$\frac{D_R}{D_R^0} = 1 - (1 - \alpha_R)\left[1 - \left\langle\frac{\tau_{bulk}}{\tau_{hyd}}\right\rangle\right]. \tag{7.3}$$

Water ^{17}O MRD studies on 11 globular proteins yield the rotational retardation factor $\langle\tau_{hyd}\rangle/\tau_{bulk} = 5.4$ (see § 5a). As discussed above, the τ_{hyd} distribution is skewed towards longer τ_{hyd} values, so that $\langle\tau_{hyd}^{-1}\rangle > \langle\tau_{hyd}\rangle^{-1}$. Taking $\langle\tau_{bulk}/\tau_{hyd}\rangle = 0.35$ and $V_{hyd} = \lambda_{hyd} A_P$, with $\lambda_{hyd} = 2$ Å for

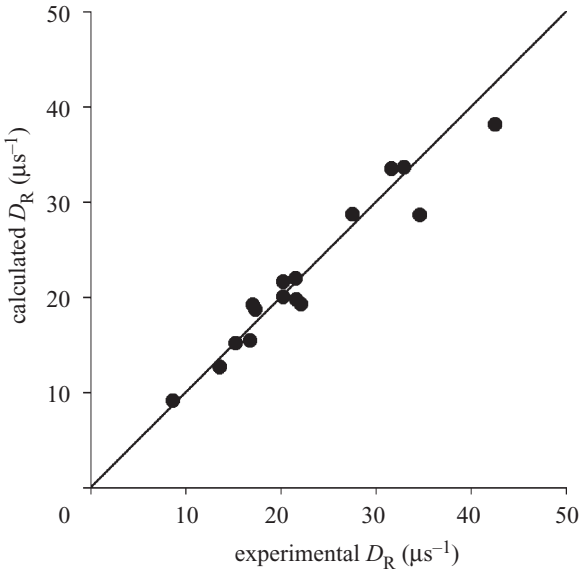

Figure 8. Correlation between rotational diffusion coefficients of proteins in H_2O at 293 K measured by ^{15}N relaxation and calculated by molecular hydrodynamics (Halle & Davidovic 2003). The data refer to 16 monomeric globular proteins in the size range of 6.5–28 kDa. The calculations were carried out with the program HYDROPRO v. 5a (Garcia de la Torre *et al.* 2000) using $\sigma_{eff} = 3.0$ Å and atomic coordinates from high-quality X-ray crystal structures. The linear correlation coefficient is 0.968 and the ratio D_R^{calc}/D_R^{expt} has a mean of 0.992 with an s.d. of 0.086.

the thickness of the hydration layer (yielding $N_{hyd} \approx 500$ for HEWL, as expected), one thus obtains $D_R/D_R^0 = 0.71$ for HEWL. The model thus accounts satisfactorily for the remaining discrepancy between experiment and molecular hydrodynamics calculations on the bare protein.

To enable *bona fide* D_R predictions by molecular hydrodynamics calculations, which are performed for a uniform solvent viscosity, the hydration effect can be simulated by using augmented atomic radii in the structural model (Halle & Davidovic 2003). Adopting the same van der Waals radius, σ_0, for all non-hydrogen atoms, one thus writes for the effective (augmented) radius, $\sigma_{eff} = \sigma_0 + \sigma_{hyd}$, where σ_{hyd} is the thickness of a hydrodynamically equivalent, rigid ($\eta \rightarrow \infty$) hydration layer that reduces the rotational diffusion coefficient of the protein by the same amount as the real mobile hydration layer. Using equation (7.3) with $\langle \tau_{bulk}/\tau_{hyd} \rangle = 0.35$, one finds $\sigma_{hyd} = 1.0$ Å, virtually independent of protein size (Halle & Davidovic 2003). The appropriate united-atom radius, weighted according to the typical 40/60 ratio of polar and non-polar atoms at the protein surface, is $\sigma_0 = 2.0$ Å. To incorporate hydration effects on protein rotational diffusion, molecular hydrodynamic calculations should therefore be carried out with an effective atomic radius, $\sigma_{eff} = 3.0$ Å. Figure 8 shows that this prediction, based on hydrodynamic theory and hydration dynamics according to MRD, is in excellent agreement with the best available experimental D_R values (from ^{15}N NMR relaxation measurements) for 16 monomeric globular proteins (Halle & Davidovic 2003). Hydration effects on translational diffusion are smaller, but can be treated in analogous fashion (Halle & Davidovic 2003).

This work was supported by the Swedish Research Council.

REFERENCES

Abragam, A. 1961 *The principles of nuclear magnetism*. Oxford: Clarendon.

Abseher, R., Schreiber, H. & Steinhauser, O. 1996 The influence of a protein on water dynamics in its vicinity investigated by molecular dynamics simulation. *Proteins* **25**, 366–378.

Akasaka, K. 1979 Intermolecular spin diffusion as a method for studying macromolecule–ligand interactions. *J. Magn. Reson.* **36**, 135–140.

Ayant, Y., Belorizky, E., Fries, P. & Rosset, J. 1977 Effet des interactions dipolaires magnétiques intermoléculaires sur la relaxation nucléaire de molécules polyatomiques dans les liquides. *J. Physique* **38**, 325–337.

Badger, J. 1997 Modeling and refinement of water molecules and disordered solvent. *Meth. Enzymol.* **277**, 344–352.

Baker, E. N. 1995 Solvent interactions with proteins as revealed by X-ray crystallographic studies. In *Protein–solvent interactions* (ed. R. B. Gregory), pp. 143–189. New York: Marcel Dekker.

Balasubramanian, S. & Bagchi, B. 2002 Slow orientational dynamics of water molecules at a micellar surface. *J. Phys. Chem.* B **106**, 3668–3672.

Bedard-Hearn, M. J., Larsen, R. E. & Schwartz, B. J. 2003 Hidden breakdown of linear response: projections of molecular motions in non-equilibrium simulations of solvation dynamics. *J. Phys. Chem.* A **107**, 4773–4777.

Bhattacharyya, K. & Bagchi, B. 2000 Slow dynamics of constrained water in complex geometries. *J. Phys. Chem.* A **104**, 10 603–10 613.

Blicharska, B., Florkowski, Z., Hennel, J. W., Held, G. & Noack, F. 1970 Investigation of protein hydration by proton spin relaxation time measurements. *Biochim. Biophys. Acta* **207**, 381–389.

Boresch, S. & Steinhauser, O. 2001 Comments on 'Anomalous dielectric relaxation of aqueous protein solutions'. *J. Phys. Chem.* A **105**, 5507–5508.

Boresch, S., Höchtl, P. & Steinhauser, O. 2000 Studying the dielectric properties of a protein solution by computer simulation. *J. Phys. Chem.* B **104**, 8743–8752.

Böttcher, C. J. F., Van Belle, O. C., Bordewijk, P. & Rip, A. 1973 *Theory of electric polarization*, vol. 2. Amsterdam: Elsevier.

Brilliantov, N. V. & Krapivsky, P. L. 1991 Stokes laws for ions in solutions with ion-induced inhomogeneity. *J. Phys. Chem.* **95**, 6055–6057.

Brunne, R. M., Liepinsh, E., Otting, G., Wüthrich, K. & Van Gunsteren, W. F. 1993 Hydration of proteins. A comparison of experimental residence times of water molecules solvating bovine pancreatic trypsin inhibitor with theoretical model calculations. *J. Mol. Biol.* **231**, 1040–1048.

Brüschweiler, R. & Wright, P. E. 1994 Water self-diffusion model for protein–water NMR cross relaxation. *Chem. Phys. Lett.* **229**, 75–81.

Buck, M., Boyd, J., Redfield, C., MacKenzie, D. A., Jeenes, D. J., Archer, D. B. & Dobson, C. M. 1995 Structural determinants of protein dynamics: analysis of ^{15}N NMR relaxation measurements for main-chain and side-chain nuclei of hen egg-white lysozyme. *Biochemistry* **34**, 4041–4055.

Byron, O. 1997 Construction of hydrodynamic bead models from high-resolution X-ray crystallographic or nuclear magnetic resonance data. *Biophys. J.* **72**, 408–415.

Caputa, K., Hennel, J. W. & Szczepkowski, T. W. 1967 Proton magnetic relaxation in protein solutions. Dependence on viscosity and temperature. In *Magnetic resonance and relaxation* (ed. R. Blinc), pp. 128–130. Amsterdam: North-Holland.

Cheng, Y.-K. & Rossky, P. J. 1998 Surface topography dependence of biomolecular hydrophobic hydration. *Nature* **392**, 696–699.

Dachwitz, E., Parak, F. & Stockhausen, M. 1989 On the dielectric relaxation of aqueous myoglobin solutions. *Ber. Bunsenges. Phys. Chem.* **93**, 1454–1458.

Daszkiewicz, O. K., Hennel, J. W., Lubas, B. & Szczepkowski, T. W. 1963 Proton magnetic relaxation and protein hydration. *Nature* **200**, 1006–1007.

Denisov, V. P. & Halle, B. 1994 Dynamics of the internal and external hydration of globular proteins. *J. Am. Chem. Soc.* **116**, 10 324–10 325.

Denisov, V. P. & Halle, B. 1996 Protein hydration dynamics in aqueous solution. *Faraday Discuss.* **103**, 227–244.

Denisov, V. P., Peters, J., Hörlein, H. D. & Halle, B. 1996 Using buried water molecules to explore the energy landscape of proteins. *Nature Struct. Biol.* **3**, 505–509.

Denisov, V. P., Venu, K., Peters, J., Hörlein, H. D. & Halle, B. 1997*a* Orientational disorder and entropy of water in protein cavities. *J. Phys. Chem.* B **101**, 9380–9389.

Denisov, V. P., Carlström, G., Venu, K. & Halle, B. 1997*b* Kinetics of DNA hydration. *J. Mol. Biol.* **268**, 118–136.

Dill, K. A. 1990 Dominant forces in protein folding. *Biochemistry* **29**, 7133–7155.

Dobson, C. M., Lian, L.-Y., Redfield, C. & Topping, K. D. 1986 Measurement of hydrogen exchange rates using 2D NMR spectroscopy. *J. Magn. Reson.* **69**, 201–209.

Drenth, J., Jansonius, J. N., Koekoek, R. & Wolthers, B. G. 1971 The structure of papain. *Adv. Protein Chem.* **25**, 79–115.

Drost-Hansen, W. 2001 Temperature effects on cell-functioning: a critical role for vicinal water. *Cell. Mol. Biol.* **47**, 865–883.

Eisenberg, D. & Kauzmann, W. 1969 *The structure and properties of water*. Oxford: Clarendon.

Ernst, R. R., Bodenhausen, G. & Wokaun, A. 1987 *Principles of nuclear magnetic resonance in one and two dimensions*. Oxford: Clarendon.

Esposito, L., Vitagliano, L., Sica, F., Sorrentino, G., Zagari, A. & Mazzarella, L. 2000 The ultrahigh resolution crystal structure of ribonuclease A containing an isoaspartyl residue: hydration and stereochemical analysis. *J. Mol. Biol.* **297**, 713–732.

Fleming, G. R. & Cho, M. 1996 Chromophore–solvent dynamics. *A. Rev. Phys. Chem.* **47**, 109–134.

Florkowski, Z., Hennel, J. W. & Blicharska, B. 1969 Apparatus for measuring proton spin relaxation time in low magnetic fields. *Nukleonika* **14**, 9–16.

Forslind, E. 1952 A theory of water. *Acta Polytechnica* **115**, 1–43.

Frank, H. S. & Evans, M. W. 1945 Free volume and entropy in condensed systems. III. Entropy in binary liquid mixtures; partial molal entropy in dilute solutions; structure and thermodynamics in aqueous electrolytes. *J. Chem. Phys.* **13**, 507–532.

Franks, F. 1981 *Polywater*. Cambridge, MA: MIT Press.

Frey, M. 1994 Water structure associated with proteins and its role in crystallization. *Acta Crystallogr.* D **50**, 663–666.

Fröhlich, H. 1958 *Theory of dielectrics*, 2nd edn. Oxford University Press.

Fujiyoshi, Y., Mitsuoka, K., de Groot, B. L., Philippsen, A., Grubmüller, H., Agre, P. & Engel, A. 2002 Structure and function of water channels. *Curr. Opin. Struct. Biol.* **12**, 509–515.

García de la Torre, J. 2001 Hydration from hydrodynamics. General considerations and applications of bead modelling to globular proteins. *Biophys. Chem.* **93**, 159–170.

García de la Torre, J. & Bloomfield, V. A. 1981 Hydrodynamic properties of complex, rigid, biological macromolecules: theory and applications. *Q. Rev. Biophys.* **14**, 81–139.

García de la Torre, J., Huertas, M. L. & Carrasco, B. 2000 Calculation of hydrodynamic properties of globular proteins from their atomic-level structure. *Biophys. J.* **78**, 719–730.

Garman, E. 2003 'Cool' crystals: macromolecular cryocrystallography and radiation damage. *Curr. Opin. Struct. Biol.* **13**, 545–551.

Garman, E. F. & Schneider, T. R. 1997 Macromolecular cryocrystallography. *J. Appl. Cryst.* **30**, 211–237.

Geiger, A., Kleene, M., Paschek, D. & Rehtanz, A. 2003 Mechanisms of the molecular mobility of water. *J. Mol. Liq.* **106**, 131–146.

Gerstein, M. & Chothia, C. 1996 Packing at the protein–water interface. *Proc. Natl Acad. Sci. USA* **93**, 10 167–10 172.

Glickson, J. D., Rowan, R., Pitner, T. P., Dadok, J., Bothner-By, A. A. & Walter, R. 1976 ^{1}H nuclear magnetic resonance double resonance study of oxytocin in aqueous solution. *Biochemistry* **15**, 1111–1119.

Gottschalk, M., Dencher, N. A. & Halle, B. 2001 Microsecond exchange of internal water molecules in bacteriorhodopsin. *J. Mol. Biol.* **311**, 605–621.

Grant, E. H. 1965 The structure of water neighboring proteins, peptides and amino acids as deduced from dielectric measurements. *Ann. N.Y. Acad. Sci.* **125**, 418–427.

Halle, B. 1998 Water in biological systems: the NMR picture. In *Hydration processes in biology* (ed. M.-C. Bellisent-Funel), pp. 233–249. Dordrecht, The Netherlands: IOS Press.

Halle, B. 2002 Flexibility and packing in proteins. *Proc. Natl Acad. Sci. USA* **99**, 1274–1279.

Halle, B. 2003 Cross-relaxation between macromolecular and solvent spins: the role of long-range dipole couplings. *J. Chem. Phys.* **119**, 12 372–12 385.

Halle, B. 2004 Biomolecular cryocrystallography: structural changes during flash-cooling. *Proc. Natl Acad. Sci. USA* **101**, 4793–4798.

Halle, B. & Davidovic, M. 2003 Biomolecular hydration: from water dynamics to hydrodynamics. *Proc. Natl Acad. Sci. USA* **100**, 12 135–12 140.

Halle, B. & Denisov, V. P. 2001 Magnetic relaxation dispersion studies of biomolecular solutions. *Meth. Enzymol.* **338**, 178–201.

Halle, B., Andersson, T., Forsén, S. & Lindman, B. 1981 Protein hydration from water oxygen-17 magnetic relaxation. *J. Am. Chem. Soc.* **103**, 500–508.

Halle, B., Denisov, V. P. & Venu, K. 1999 Multinuclear relaxation dispersion studies of protein hydration. In *Biological magnetic resonance*, vol. 17 (ed. N. R. Krishna & L. J. Berliner), pp. 419–484. New York: Kluwer/Plenum.

Halle, B., Denisov, V. P., Modig, K. & Davidovic. M. 2004 Protein conformational transitions as seen from the solvent: magnetic relaxation dispersion studies of water, cosolvent and denaturant interactions with non-native proteins. In *Handbook of protein folding*, vol. I (ed. J. Buchner & T. Kiefhaber). Weinheim, Germany: Wiley–VCH. (In the press.)

Harpaz, Y., Gerstein, M. & Chothia, C. 1994 Volume changes on protein folding. *Structure* **2**, 641–649.

Hazlewood, C. F. 2001 Information forgotten or overlooked: fundamental flaws in the conventional view of the living cell. *Cell. Mol. Biol.* **47**, 959–970.

Henchman, R. H. & McCammon, J. A. 2002 Structural and dynamic properties of water around acetylcholinesterase. *Protein Sci.* **11**, 2080–2090.

Impey, R. W., Madden, P. A. & McDonald, I. R. 1983 Hydration and mobility of ions in solution. *J. Phys. Chem.* **87**, 5071–5083.

Islam, S. A. & Weaver, D. L. 1990 Molecular interactions in protein crystals: solvent accessible surface and stability. *Proteins* **8**, 1–5.

Jacobson, B. 1953 Hydration structure of deoxyribonucleic acid and its physico-chemical properties. *Nature* **172**, 666–667.

Jacobson, B., Anderson, W. A. & Arnold, J. T. 1954 A proton magnetic resonance study of the hydration of deoxyribonucleic acid. *Nature* **173**, 772–773.

Jimenez, R., Fleming, G. R., Kumar, P. V. & Maroncelli, M. 1994 Femtosecond solvation dynamics of water. *Nature* **369**, 471–473.

Kaatze, U. 1989 Complex permittivity of water as a function of frequency and temperature. *J. Chem. Engng Data* **34**, 371–374.

Kauzmann, W. 1959 Some factors in the interpretation of protein denaturation. *Adv. Protein Chem.* **14**, 1–63.

Kimmich, R. & Noack, F. 1970*a* Messung kurzer Kernspinrelaxationszeiten in schwachen Magnetfeldern bei kleinen Probenvolumina. *Z. Angew. Phys.* **29**, 248–252.

Kimmich, R. & Noack, F. 1970*b* Zur deutung der kernmagnetischen relaxation in proteinlösungen. *Z. Naturforsch.* **25a**, 1680–1684.

Klotz, I. M. 1958 Protein hydration and behavior. *Science* **128**, 815–822.

Knocks, A. & Weingärtner, H. 2001 The dielectric spectrum of ubiquitin in aqueous solution. *J. Phys. Chem.* B **105**, 3635–3638.

Koenig, S. H. & Schillinger, W. E. 1969 Nuclear magnetic relaxation dispersion in protein solutions. I. Apotransferrin. *J. Biol. Chem.* **244**, 3283–3289.

Korzhnev, D. M., Billeter, M., Arseniev, A. S. & Orekhov, V. Y. 2001 NMR studies of Brownian tumbling and internal motions in proteins. *Prog. NMR Spectrosc.* **38**, 197–266.

Kovacs, H., Mark, A. E. & Van Gunsteren, W. F. 1997 Solvent structure at a hydrophobic protein surface. *Proteins* **27**, 395–404.

Kriminski, S., Kazmierczak, M. & Thorne, R. E. 2003 Heat transfer from protein crystals: implications for flash-cooling and X-ray beam heating. *Acta Crystallogr.* D **59**, 697–708.

Kuntz, I. D. & Kauzmann, W. 1974 Hydration of proteins and polypeptides. *Adv. Protein Chem.* **28**, 239–345.

Landau, L. D. & Lifshitz, E. M. 1959 *Fluid mechanics*. Oxford: Pergamon.

Lanyi, J. K. 2000 Molecular mechanism of ion transport in bacteriorhodopsin: insights from crystallographic, spectroscopic, kinetic, and mutational studies. *J. Phys. Chem.* B **104**, 11 441–11 448.

Ling, G. N. 1962 *A physical theory of the living state: the association–induction hypothesis*. New York: Blaisdell Publishing Co.

Luecke, H., Schobert, B., Richter, H.-T., Cartailler, J.-P. & Lanyi, J. K. 1999 Structure of bacteriorhodopsin at 1.55 Å resolution. *J. Mol. Biol.* **291**, 899–911.

Luise, A., Falconi, M. & Desideri, A. 2000 Molecular dynamics simulation of solvated azurin: correlation between surface solvent accessibility and water residence times. *Proteins* **39**, 56–67.

Makarov, V. A., Andrews, B. K., Smith, P. E. & Pettitt, B. M. 2000 Residence times of water molecules in the hydration sites of myoglobin. *Biophys. J.* **79**, 2966–2974.

Marchi, M., Sterpone, F. & Ceccarelli, M. 2002 Water rotational relaxation and diffusion in hydrated lysozyme. *J. Am. Chem. Soc.* **124**, 6787–6791.

Merzel, F. & Smith, J. C. 2002 Is the first hydration shell of lysozyme of higher density than bulk water? *Proc. Natl Acad. Sci. USA* **99**, 5378–5383.

Meyer, E. 1992 Internal water molecules and H-bonding in biological macromolecules: a review of structural features with functional implications. *Protein Sci.* **1**, 1543–1562.

Miura, N., Asaka, N., Shinyashiki, N. & Mashimo, S. 1994 Microwave dielectric study on bound water of globule proteins in aqueous solution. *Biopolymers* **34**, 357–364.

Modig, K. & Halle, B. 2002 Proton magnetic shielding tensor in liquid water. *J. Am. Chem. Soc.* **124**, 12 031–12 041.

Modig, K., Rademacher, M., Lücke, C. & Halle, B. 2003 Water dynamics in the large cavity of three lipid-binding proteins monitored by ^{17}O magnetic relaxation dispersion. *J. Mol. Biol.* **332**, 965–977.

Modig, K., Liepinsh, E., Otting, G. & Halle, B. 2004 Dynamics of protein and peptide hydration. *J. Am. Chem. Soc.* **126**, 102–114.

Murphy, L. R., Matubayasi, N., Payne, V. A. & Levy, R. M. 1998 Protein hydration and unfolding: insights from experimental partial specific volumes and unfolded protein models. *Fold. Design* **3**, 105–118.

Nakasako, M. 1999 Large-scale networks of hydration water molecules around bovine β-trypsin revealed by cryogenic X-ray crystal structure analysis. *J. Mol. Biol.* **289**, 547–564.

Nandi, N. & Bagchi, B. 1997 Dielectric relaxation of biological water. *J. Phys. Chem.* B **101**, 10 954–10 961.

Nandi, N. & Bagchi, B. 1998 Anomalous dielectric relaxation of aqueous protein solutions. *J. Phys. Chem.* A **102**, 8217–8221.

Nandi, N., Bhattacharyya, K. & Bagchi, B. 2000 Dielectric relaxation and solvation dynamics of water in complex chemical and biological systems. *Chem. Rev.* **100**, 2013–2045.

Neuhaus, D. & Williamson, M. P. 2000 *The nuclear Overhauser effect in structural and conformational analysis*, 2nd edn. New York: Wiley–VCH.

Ohlendorf, D. H. 1994 Accuracy of refined protein structures. II. Comparison of four independently refined models of human interleukin 1β. *Acta Crystallogr.* D **50**, 808–812.

Oleinikova, A., Sasisanker, P. & Weingärtner, H. 2004 What can really be learned from dielectric spectroscopy of protein solutions? A case study of ribonuclease A. *J. Phys. Chem.* B. (In the press.) (DOI 10.1021/jp049618b.)

Oncley, J. L. 1938 Studies on the dielectric properties of protein solutions. I. Carboxy-hemoglobin. *J. Am. Chem. Soc.* **60**, 1115–1123.

Otting, G. 1997 NMR studies of water bound to biological molecules. *Prog. NMR Spectrosc.* **31**, 259–285.

Otting, G. & Liepinsh, E. 1995 Protein hydration viewed by high-resolution NMR spectroscopy: implications for magnetic resonance image contrast. *Acc. Chem. Res.* **28**, 171–177.

Otting, G. & Wüthrich, K. 1989 Studies of protein hydration in aqueous solution by direct NMR observation of individual protein-bound water molecules. *J. Am. Chem. Soc.* **111**, 1871–1875.

Otting, G., Liepinsh, E. & Wüthrich, K. 1991*a* Protein hydration in aqueous solution. *Science* **254**, 974–980.

Otting, G., Liepinsh, E., Farmer, B. T. & Wüthrich, K. 1991*b* Protein hydration studied with homonuclear 3D ^{1}H NMR experiments. *J. Biomol. NMR* **1**, 209–215.

Otting, G., Liepinsh, E. & Wüthrich, K. 1992 Polypeptide hydration in mixed solvents at low temperatures. *J. Am. Chem. Soc.* **114**, 7093–7095.

Pal, S. K. & Zewail, A. H. 2004 Dynamics of water in biological recognition. *Chem. Rev.* **104**, 2099–2123.

Pal, S. K., Peon, J., Bagchi, B. & Zewail, A. H. 2002*a* Biological water: femtosecond dynamics of macromolecular hydration. *J. Phys. Chem.* B **106**, 12 376–12 395.

Pal, S. K., Peon, J. & Zewail, A. H. 2002*b* Biological water at the protein surface: dynamical solvation probed directly with femtosecond resolution. *Proc. Natl Acad. Sci. USA* **99**, 1763–1768.

Pal, S. K., Peon, J. & Zewail, A. H. 2002*c* Ultrafast surface hydration dynamics and expression of protein functionality: α-chymotrypsin. *Proc. Natl Acad. Sci. USA* **99**, 15 297–15 302.

Pal, S., Balasubramanian, S. & Bagchi, B. 2002*d* Temperature dependence of water dynamics at an aqueous micellar surface: atomistic molecular dynamics simulation studies of a complex system. *J. Chem. Phys.* **117**, 2852–2859.

Papazyan, A. & Maroncelli, M. 1995 Rotational dielectric friction and dipole solvation: tests of theory based on simulations of simple model solutions. *J. Chem. Phys.* **102**, 2888–2919.

Peon, J., Pal, S. K. & Zewail, A. H. 2002 Hydration at the surface of the protein monellin: dynamics with femtosecond resolution. *Proc. Natl Acad. Sci. USA* **99**, 10 964–10 969.

Perrin, F. 1936 Mouvement Brownien d'un ellipsoide (II). Rotation libre et dépolarisation des fluorescences, translation et diffusion de molécules ellipsoidales. *J. Phys. Radium* **7**, 1–11.

Pethig, R. 1992 Protein–water interactions determined by dielectric methods. *A. Rev. Phys. Chem.* **43**, 177–205.

Pethig, R. 1995 Dielectric studies of protein hydration. In *Protein–solvent interactions* (ed. R. B. Gregory), pp. 265–288. New York: Marcel Dekker.

Pitner, T. P., Glickson, J. D., Dadok, J. & Marshall, G. R. 1974 Solvent exposure of specific nuclei of angiotensin II determined by NMR solvent saturation method. *Nature* **250**, 582–584.

Quiocho, F. A. & Lipscomb, W. N. 1971 Carboxypeptidase A: a protein and an enzyme. *Adv. Protein Chem.* **25**, 1–78.

Redfield, A. G., Fite, W. & Bleich, H. E. 1968 Precision high speed current regulators for occasionally switched inductive loads. *Rev. Sci. Instrum.* **39**, 710–715.

Rupley, J. A. & Careri, G. 1991 Protein hydration and function. *Adv. Protein Chem.* **41**, 37–172.

Samoilov, O. Y. 1957 *Struktura vodnyh rastvorov elektrolitov i gidrataciya ionov*. Moscow: Academic Science.

Schwarz, G. 1967 On dielectric relaxation due to chemical rate processes. *J. Phys. Chem.* **71**, 4021–4030.

Schwartz, A. L. & Cutnell, J. D. 1983 One- and two-dimensional NMR studies of exchanging amide protons in glutathione. *J. Magn. Reson.* **53**, 398–411.

Seki, Y., Tomizawa, T., Khechinashvili, N. N. & Soda, K. 2002 Contribution of solvent water to the solution X-ray scattering profile of proteins. *Biophys. Chem.* **95**, 235–252.

Shen, X. & Knutson, J. R. 2001 Subpicosecond fluorescence spectra of tryptophan in water. *J. Phys. Chem.* B **105**, 6260–6265.

Snook, I. K. & Henderson, D. 1978 Monte Carlo study of a hard-sphere fluid near a hard wall. *J. Chem. Phys.* **68**, 2134–2139.

Squire, P. G. & Himmel, M. E. 1979 Hydrodynamics and protein hydration. *Arch. Biochem. Biophys.* **196**, 165–177.

Stoesz, J. D., Redfield, A. G. & Malinowski, D. 1978 Cross relaxation and spin diffusion effects on the proton NMR of biopolymers in H_2O. *FEBS Lett.* **91**, 320–324.

Svergun, D. I., Richard, S., Koch, M. H. J., Sayers, Z., Kuprin, S. & Zaccai, G. 1998 Protein hydration in solution: experimental observation by X-ray and neutron scattering. *Proc. Natl Acad. Sci. USA* **95**, 2267–2272.

Teeter, M. M., Yamano, A., Stec, B. & Mohanty, U. 2001 On the nature of a glassy state of matter in a hydrated protein: relation to protein function. *Proc. Natl Acad. Sci. USA* **98**, 11 242–11 247.

Van de Ven, F. J. M. & Hilbers, C. W. 1988 Sequential resonance assignments as a basis for the determination of a three-dimensional structure of protein E-L30 of *Escherichia coli*. *J. Mol. Biol.* **192**, 419–441.

Van De Ven, F. J. M., Janssen, H. G. J. M., Gräslund, A. & Hilbers, C. W. 1988 Chemically relayed nuclear Overhauser effects. Connectivities between resonances of non-exchangeable protons and water. *J. Magn. Reson.* **79**, 221–235.

Venable, R. M. & Pastor, R. W. 1988 Frictional models for stochastic simulations of proteins. *Biopolymers* **27**, 1001–1014.

Wei, Y.-Z., Kumbharkhane, A. C., Sadeghi, M., Sage, J. T., Tian, W. D., Champion, P. M., Sridhar, S. & McDonald, M. J. 1994 Protein hydration investigations with high-frequency dielectric spectroscopy. *J. Phys. Chem.* **98**, 6644–6651.

Williams, M. A., Goodfellow, J. M. & Thornton, J. M. 1994 Buried waters and internal cavities in monomeric proteins. *Protein Sci.* **3**, 1224–1235.

Wlodawer, A., Walter, J., Huber, R. & Sjölin, L. 1984 Structure of bovine pancreatic trypsin inhibitor. Results of joint neutron and X-ray refinement of crystal form II. *J. Mol. Biol.* **180**, 301–329.

Wlodawer, A., Nachman, J., Gilliland, G. L., Gallagher, W. & Woodward, C. 1987 Structure of form III crystals of bovine pancreatic trypsin inhibitor. *J. Mol. Biol.* **198**, 469–480.

Wolynes, P. G. 1980 Dynamics of electrolyte solutions. *A. Rev. Phys. Chem.* **31**, 345–376.

Zhao, H. & Pearlstein, A. J. 2002 Stokes-flow computation of the diffusion coefficient and rotational diffusion tensor of lysozyme, a globular protein. *Phys. Fluids* **14**, 2376–2387.

Zwanzig, R. 2001 *Non-equilibrium statistical mechanics*. New York: Oxford University Press.

Discussion

J. R. Helliwell (*Department of Chemistry, University of Manchester, Manchester, UK*). I have a few comments.

(i) You criticize the use by crystallographers of the words 'bound solvent'. As crystallographers, we could say that, for example, Henry VIII was married all his life, we cannot say he was married six times! Most of the time one or more waters are bound at one site is what we mean by a 'bound water molecule'.

(ii) As Jeremy Smith stated in his title, you also in your abstract refer to 'perturbation of water'. It seems you emphasize this role particularly as vital to life. If we take examples of protein–ligand recognition, water is versatile, i.e. is willing to be non-perturbed when it is needed and be perturbed (i.e. displaced) when it is needed. See, for example, the case of lectin saccharide crystal structures; in con A, waters are displaced (Gilboa & Helliwell 2001); in peanut lectin, two waters help 'glue' the sugar to the protein (Pratap *et al*. 2001). The versatility of water is then a key facet for life.

(iii) If one is anxious about cryo-artefacts of a 100 K protein crystal structure, it is often possible to check with a crystal structure study at room temperature. If a crystal structure at room temperature is not possible (e.g. as a result of X-ray damage), then case studies document the bounds or range of structural change (e.g. Deacon *et al.* 1997) that occur on freezing. Such changes produce more multiple-occupancy side chains and, associated with these, bound-water movements. Indeed, I agree, extrapolation to *in vivo* should take account of such 'artefactual' details or, best of all, as I say above, for the crystallographer to determine a room-temperature protein crystal structure as well.

B. Halle.

(i) Two distinct issues are involved here. First, diffraction intensities measured on an equilibrium ensemble of protein molecules in a crystal provide no information whatsoever about the rates of molecular motions. Diffraction data should therefore not be discussed in terms of 'dynamics', which refers to motion. Second, the fact that water molecules near the protein surface are resolved in the electron density map, whereas more remote water molecules are not, does not, as often implied, mean that water molecules at the surface are 'tightly bound'. The relative visibility of these water molecules is a trivial consequence of the crystalline order of protein molecules and the space-filling capacity of water molecules. Consider a crystalline array of large hard spheres surrounded by spatially unconstrained small hard spheres. Merely by excluding volume, the large sphere induces correlations in the positions of nearby small spheres, thereby enhancing their crystallographic visibility. Because there are no attractive interactions in the system, it is incorrect to describe these positionally ordered solvent spheres as 'tightly bound'. If the large particle has a rugged surface (such as a protein), it also induces lateral correlations within the first solvent layer.

(ii) The role of water molecules in modulating the affinity, selectivity and kinetics of protein–ligand, protein–protein and protein–DNA associations was not addressed directly in my contribution. To make progress in this important area, the structural, energetic and dynamic properties of hydration water molecules need to be investigated. Depending on the nature of the binding site (for example, a fully exposed site versus a deep invagination or cavity), it may be more or less convenient to characterize these properties in terms of the perturbation of the corresponding bulk water properties.

(iii) The problem with cryostructures is that they portray a thermally inhomogeneous protein structure, where different degrees of freedom have been equilibrated at different temperatures. The biological relevance can be assessed only by experiments performed at, or near, the physiological temperature. This is done for less than 10% of the protein structures currently being deposited in the Protein Data Bank.

A. Kornyshev (*Department of Chemistry, Imperial College London, London, UK*). Can a Stokes shift probe be inserted into the channel of bacteriorhodopsin and the dynamics of water resolvation measured?

B. Halle. The problem with the DSS method as applied to protein hydration is that it cannot distinguish probe–water interactions from probe–protein interactions. A DSS experiment on a probe located in the proton translocation channel of bacteriorhodopsin would probably say more about the relative motions of the probe and the several nearby ionic side chains than about the water molecules in the channel.

J. B. F. N. Engberts (*Physical Organic Chemistry Unit, University of Groningen, Groningen, The Netherlands*). I would like to add another factor to the discussion. In living cells, proteins and, in particular, enzymes do not function in dilute aqueous solutions but rather in the cytosol containing up to 500 g l^{-1} of dissolved biomolecules. These aqueous solutions are thermodynamically far from ideal. In the cytosol there is *no* bulk water (emphasized by P. Ball in his *Biography of water*). This situation is beautifully illustrated by the finding that some proteins fold only in the cytosol and *not* in dilute aqueous solutions. What are the consequences for the dynamics of protein hydration in the living cell?

B. Halle. The principal effects of macromolecular crowding in intracellular environments are probably: (i) to stabilize folded proteins against unfolding by effectively prohibiting highly extended conformations; and (ii) to promote biomolecular association by increasing the free volume available to other macromolecules (a phenomenon that, in the colloid field, is known as the depletion interaction). These purely entropic mechanisms do not affect small molecules like water. The structure, energetics and kinetics of protein hydration are more likely to be altered by various cosolvents, some of which are produced at very high concentrations in response to environmental stress. The categorical statement that there is no bulk water in the cytosol, is no more profound or useful than the similarly fundamentalist claim that there are no isolated systems in the universe. If we allow a 10% variation in single-molecule properties, such as the rotational correlation time, then even a typical protein crystal, with 60% protein by volume, contains a significant amount of bulk water.

Additional references

Ball, P. 2000 *H_2O: a biography of water*. London: Orion Publ. Co.

Deacon, A., Gleichmann, T., Kalb, A. J., Price, H., Raftery, J., Bradbrook, G., Yariv, J. & Helliwell, J. R. 1997 The structure of concanavalin A and its bound solvent determined with small-molecule accuracy at 0.94 Ångström resolution. *J. Chem. Soc. Faraday Trans.* **93**, 4305–4312.

Gilboa, A. J. K. & Helliwell, J. R. 2001 Concavalin A. In *Handbook of metalloproteins* (ed. A. Messerschmidt, R. Huber, K. Wieghardt & T. Poulos), pp. 963–972. New York: J. Wiley & Sons.

Pratap, J. V., Bradbrook, G. M., Reddy, G. B., Surolia, A., Raftery, J., Helliwell, J. R. & Vijayan, M. 2001 The combination of molecular dynamics with crystallography for elucidating protein–ligand interactions: a case study involving peanut lectin complexes with T-antigen and lactose. *Acta Crystallogr.* D **57**, 1584–1594. (DOI 10.1107/S090744 4901011957.)

GLOSSARY

^{17}O: oxygen-17
BPTI: bovine pancreatic trypsin inhibitor
DRS: dielectric relaxation spectroscopy
DSS: dynamic Stokes shift
HEWL: hen egg-white lysozyme
MRD: magnetic relaxation dispersion
NMR: nuclear magnetic resonance
NOE: nuclear Overhauser effect
NOESY: NOE spectroscopy
ROESY: rotating-frame NOE spectroscopy